

10. PALYNOLOGY AND DINOFLAGELLATE BIOSTRATIGRAPHY OF UPPER CENOZOIC SEDIMENTS FROM SITES 898 AND 900, IBERIA ABYSSAL PLAIN¹

Francine M.G. McCarthy² and Peta J. Mudie³

ABSTRACT

Palynomorphs were analyzed from 58 samples from ODP Leg 149 Hole 898A to establish an upper Cenozoic dinoflagellate cyst biostratigraphy for the Iberia Abyssal Plain. Five informal dinocyst biozones are defined based on the stratigraphic ranges of 75 dinocyst morphotypes identified from these sediments. These biozones are compared with dinocyst assemblages identified from a smaller number of samples (16) in Hole 900A, 43 km to the east at the base of the continental rise. A number of the dinocyst biozones defined in Hole 898A can be identified in sediments of equivalent age in Hole 900A, which differs mainly in the low numbers of protoperidinioid (congruentidioid) dinocysts and pollen. There are, however, significant differences between the Pliocene-Pleistocene sequences from these two sites, due to the abundant influx of terrigenous sediments to Site 898 with the beginning of turbidite sedimentation. Turbidite sediments can be identified palynologically by their ratio of marine palynomorphs (dinoflagellate cysts and acritarchs) vs. terrestrial palynomorphs (pollen and spores). This ratio (D:P) provides insight into the provenance of sediments on the Iberia Abyssal Plain while simultaneously providing paleoenvironmental information, allowing changes in depositional and erosional patterns in the eastern Iberia Abyssal Plain to be directly related to large-scale paleoclimatic and paleoceanographic changes in the temperate-subtropical eastern North Atlantic.

INTRODUCTION

Four sites on the Iberia Abyssal Plain were cored during Leg 149 of the Ocean Drilling Program (ODP). Two sites were selected for palynological study of the recovered Miocene to Pleistocene sediments: Hole 898A at 41°41.100'N, 12°7.380'W, and Hole 900A at 41°40.994'N, 11°36.252'W. Site 898 is located in the eastern part of the Iberia Abyssal Plain at a water depth of 5279.0 m, and Site 900 is 43 km east of Site 898, in 5036.8 m of water near the base of the continental rise.

The Iberia Abyssal Plain is overlain by surface water from the North Atlantic (NAC) and Azores (AC) currents and by Mediterranean Water (MW) at depths of 0.5 to 3 km (Fairbridge, 1966; Sy, 1988; Fig. 1). The surface water off Iberia, formerly called the Portugal Current (Dietrich, 1963), is now known to be formed intermittently by southerly and easterly meanders of the NAC and AC, respectively (Sy, 1988). The water flows southeast to join the North Equatorial Current on the southern edge of the North Atlantic subtropical gyre, at about 20°N. Summer sea surface temperature and salinity are ~18°-20°C and 35.5‰-36.5‰, respectively (Fairbridge, 1966; Pickard and Emery, 1982). The wedge of Mediterranean overflow water has a temperature and salinity of ~11°-13°C and 36.5‰-37‰, respectively. Recent detailed studies (Sy, 1988) show that the MW flows both south and northwest off Spain, with its inshore boundaries being constrained by the locations of the meandering NAC and AC branches.

There have been a few previous studies of Miocene to Quaternary stratigraphic distributions of dinoflagellate cysts (dinocysts) in the warm temperate and subtropical North Atlantic Ocean (Harland, 1979; Edwards, 1984; Williams and Bujak, 1985; Mudie, 1987; de Vernal et al., 1992), in the Gulf of Mexico (Wrenn and Kokinos,

1986), and in the Mediterranean (Habib, 1971; Jan du Chêne, 1977; Corradini and Biffi, 1988; Powell, 1986a,b,c, 1992; Londeix et al., 1992; Benzakour, 1992; Aksu et al., 1995). Many of these studies were done on sections with poorly constrained age control (deep sea sites), or poor palynomorph preservation and much reworking (onshore Mediterranean sites; Powell, pers. comm., 1994). Consequently, there are many difficulties in studying the palynological assemblages from the Iberia Abyssal Plain, where turbidites are a major sediment source (Shipboard Scientific Party, 1994a), sea-surface temperatures and salinities are variable, and where palynomorphs from the Mediterranean Sea may be transported into the North Atlantic via Mediterranean overflow water. Despite these difficulties, the stratigraphic ranges of dinocysts published in previous works permit the erection of a preliminary biostratigraphic zonation, and because organic-walled dinoflagellates, as a group, are euryhaline and eurythermal, their cysts are useful microfossils in sediments that contain a sparse calcareous microfossil record. This is particularly relevant to the study of the Iberia Abyssal Plain, where some intervals lack biostratigraphically diagnostic calcareous nannofossils or planktonic foraminifers.

The widespread distribution of dinocysts and acritarchs, as well as the presence of terrigenous pollen and spores transported into the oceans, make palynomorphs useful paleoecological indicators in marine sediments. During the planktonic motile stage, most dinoflagellates live in the photic zone, so surface water conditions can be reconstructed from assemblages of the organic-walled resting cysts in the underlying sediment. Several studies have successfully correlated the distribution of dinocysts in surface sediments of the North Atlantic region with overlying surface water masses (Harland, 1977; Wall et al., 1977; Harland, 1983; Turon, 1984; Mudie and Short, 1985; Mudie, 1987; Dale, 1976; Dodge and Harland, 1991; Dodge, 1994). Quantitative methods have also been developed (Mudie et al., 1990; Edwards et al., 1991; Mudie, 1992) to apply these ecological correlations to paleoclimatic reconstruction. Pollen and terrestrial spores provide insights into atmospheric circulation (Mudie and McCarthy, 1994), and these palynomorphs can be used as tracers for the transport of fine-grained terrigenous sediments onto the abyssal plain, either by downslope mass wasting (turbidites), ice-rafting, or eolian transport. The importance of downslope mass transport in this region

¹Whitmarsh, R.B., Sawyer, D.S., Klaus, A., and Masson, D.G. (Eds.), 1996. *Proc. ODP, Sci. Results*, 149: College Station, TX (Ocean Drilling Program).

²Department of Earth Sciences, Brock University, St. Catharines, Ontario L2S 3A1, Canada. francine@eraton.geol.brocku.ca

³Geological Survey Canada, Atlantic Geoscience Centre, Box 1006, Dartmouth, Nova Scotia B2Y 4A2, Canada.

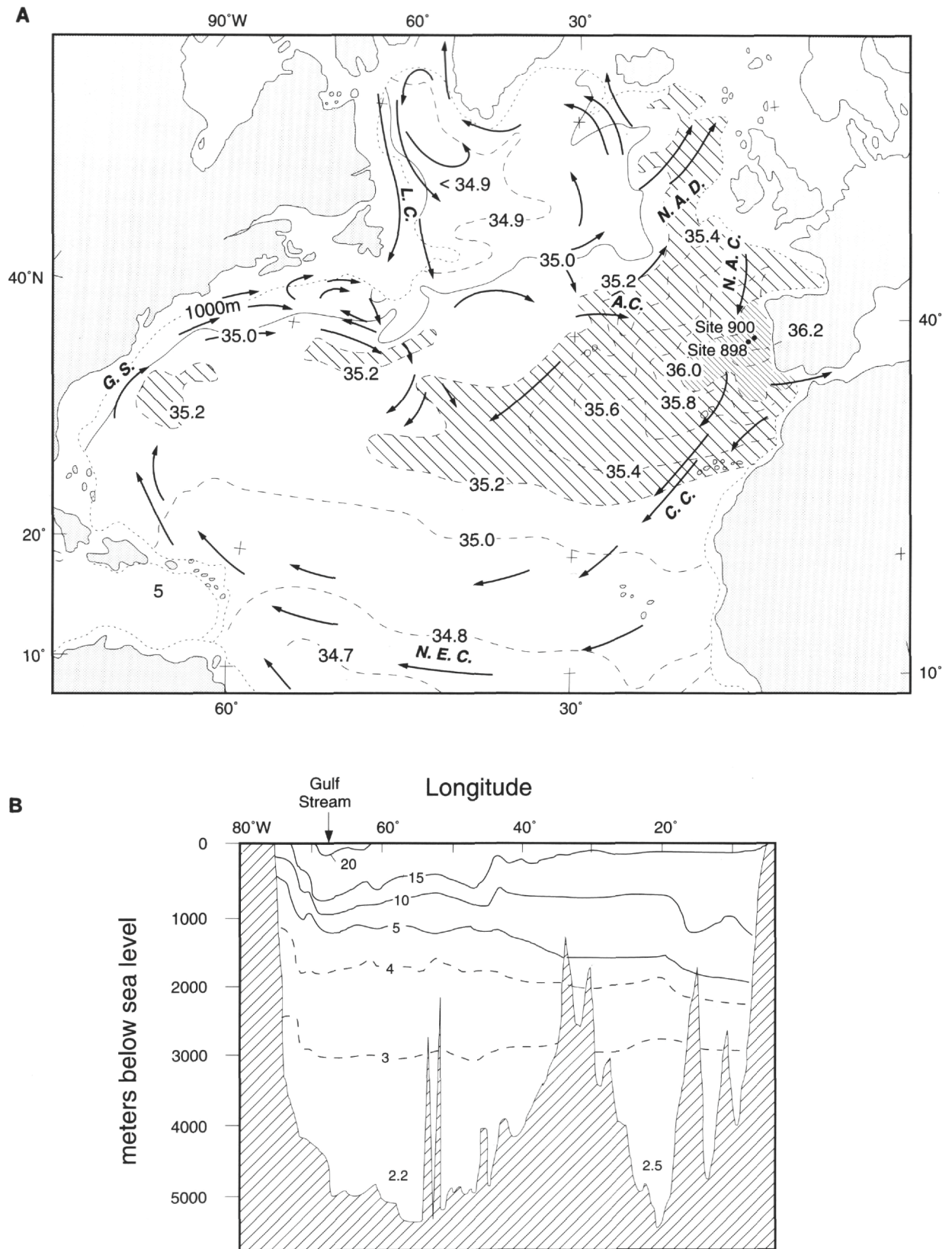


Figure 1. Distributions of currents, temperature, and salinity in the North Atlantic Ocean (modified from Dietrich, 1963). A. Salinity (‰) at 1000 m depth, and surface currents (G.S. = Gulf Stream, L.C. = Labrador Current, N.A.D. = North Atlantic Drift, A.C. = Azores Current, N.A.C. = North Atlantic Current, C.C. = Canaries Current, N.E.C. = North Equatorial Current). Hatching delimits areas of high salinity >35‰ (coarse) and >36‰ (fine), showing the distribution of Mediterranean overflow water at intermediate depths. B. Cross section of temperature (°C) at 40°N in the North Atlantic.

is highlighted by the presence of calcareous microfossils through much of the Neogene through Quaternary sequence in Holes 898A and 900A, despite these sites being located below the carbonate compensation depth for much of that period.

The location of Sites 898 and 900 allows the study of the impact of large-scale circulation and sea level changes on the Iberia Abyssal Plain through the late Cenozoic, in addition to regional tectonic effects associated with the closing of the Paratethys Ocean during the Messinian (5.3–4.86 Ma), the northward drift of the Iberian Peninsula, and the opening of the Strait of Gibraltar during the early Zanclean stage, ~4.86–4.6 Ma (Shipboard Scientific Party, 1994a). The palynological record permits examination of surface water conditions at the boundary between the oceanic and neritic environments, and the reconstruction of the position of the temperate and subtropical surface waters and of the Mediterranean overflow waters through time on the Iberian margin. Sedimentation at Sites 898 and 900 would also have been affected by these oceanographic changes, as suggested by the high frequency of turbidites in the late Pliocene and Quaternary sediments.

Scientific Objectives

The objectives of the palynological study were:

1. To document the palynomorphs present in late Cenozoic sediments recovered in Holes 898A and 900A, and to describe the character of the dinocyst assemblages studied.
2. To establish a dinoflagellate cyst biostratigraphy for Holes 898A and 900A calibrated to the calcareous nannofossil and planktonic foraminiferal chronostratigraphic data.
3. To interpret early Miocene through middle Pleistocene paleoclimatic and paleoceanographic conditions from the record of marine and terrestrial palynomorphs and to relate these paleoenvironmental conditions to depositional and erosional processes in the eastern Iberia Abyssal Plain.

Lithostratigraphy and Chronostratigraphy of Holes 898A and 900A

The Shipboard Scientific Party (1994b) identified two major lithologic units in Hole 898A. Unit I (0–163.4 mbsf, Cores 1H to 18X-4, 75 cm) consists of silty clay to clayey silt, silt, and fine sand with nannofossil clay. This unit is dominated by greenish black siliciclastic turbidites, which are mostly capped by light gray nannofossil-rich hemipelagic/pelagic sediments. Unit I was assigned a Pleistocene through late Pliocene age by the Shipboard Scientific Party (Table 1). This age assignment has been supported by shorebased studies of planktonic foraminifers, where the presence of *Globorotalia truncatulinoides* (D'Orbigny) in Samples 149-898A-17X-6, 33–35 cm and 149-898A-18X-1, 148–150 cm indicates a late Pliocene to Pleistocene age, N22, (Gervais, this volume).

A major unconformity, which correlates with acoustic formation boundary 1 A/IB, separates Unit I from Unit II. The sediments of Unit II were assigned an age of middle Miocene-late Oligocene, thus the hiatus appears to span 10 m.y. (Shipboard Scientific Party, 1994b). Subunit IIA (163.4–172.2 mbsf) is a thin, intensely bioturbated sequence of brown silty clay, nannofossil clay, and nannofossil ooze, interpreted as pelagic and hemipelagic deposits of middle Miocene age. Subunit IIB (172.2–339.7 mbsf) consists of light greenish gray, fine-grained, carbonate-rich turbidites and contourites, and darker, carbonate-poor, hemipelagic/pelagic deposits of middle Miocene to late Oligocene age.

Two major lithologic units were also identified at Site 900, separated by a hiatus spanning about 4 m.y. in the middle late Miocene, that correlate with a regional angular unconformity on seismic reflection profiles (Shipboard Scientific Party, 1994c). Subunit IA (0–67.2 mbsf) consists of Pleistocene to upper Pliocene mud-dominated tur-

bidites and hemipelagic/pelagic sediment. Subunit IB (67.2–96.0 mbsf) is hemipelagic/pelagic sediment of late Pliocene to late Miocene age. Subunit IC (96.0–181.5 mbsf) consists of upper Miocene to middle Miocene mud-dominated turbidites and hemipelagic/pelagic sediment. Despite the presence of turbidites as well as hemipelagic and pelagic facies, at Site 900 Unit I contains little siliciclastic sediment compared to Sites 897, 898, and 899. Sediment accumulation rates through most of Site 900 Unit I are also much lower (~1/3) than in Unit I at other sites on the Iberia Abyssal Plain (Milkert et al., this volume). Subunit IIA (181.5–234.3 mbsf) consists of lower Miocene turbidites and contourites and hemipelagic/pelagic sediments. Subunit IIB (234.3–748.9 mbsf) consists of lower Miocene to Paleocene sediments, possibly including turbidites reworked by contour currents. Sediment accumulation rates in Unit II are comparable to rates in units of the same age at other sites on the Iberia Abyssal Plain (Shipboard Scientific Party, 1994c).

METHODS

Samples of approximately 5 cm³ volume were disaggregated for 12–24 hours using dilute Calgon. Samples were then treated with 10% HCl, and *Lycopodium* tablets (Stockmarr, 1971) were added prior to sieving at 150 and 10 µm mesh sizes. The samples were then treated with hot concentrated HCl and HF (48–52%) to remove carbonates and silicates, respectively. Residues were stained with safranin-O and mounted in glycerine jelly. A minimum of 2 slides was made per sample; the slides were scanned using a Leitz Orthoplan microscope at Brock University and a Zeiss Universal microscope with Normarski interference contrast at the Bedford Institute of Oceanography. Palynomorph abundances were estimated based on counts of between 20 and 200 dinocysts, and absolute palynomorph concentrations were estimated using the ratio of spiked *Lycopodium* spores to palynomorphs counted in analysis. Photographs were taken at the Bedford Institute of Oceanography using a Zeiss Universal microscope and 35 mm camera with Kodacolor 100 film. The locations of photographed palynomorphs on slides curated at the Bedford Institute are indicated by England Finder references.

RESULTS OF THE PALYNOLOGICAL ANALYSIS

Calcareous nannofossils, and to a lesser extent, planktonic foraminifers, provided the shipboard biostratigraphic control for Holes 898A and 900A (Shipboard Scientific Party, 1994b, c). Current biostratigraphic zonations, including additional shore-based analyses, are shown in the dinocyst range charts (Fig. 2; Tables 1, 2), highlighting discrepancies between the two calcareous microfossil groups. Dinocyst stratigraphy provides additional biostratigraphic information for these holes. Although there is no standard dinoflagellate cyst zonation for the late Cenozoic, there have been several detailed studies of Miocene to Pleistocene dinoflagellate palynostratigraphies from the North Atlantic Ocean (Harland, 1979, 1989; Williams and Bujak, 1985; Mudie, 1987, 1989; Head et al. 1989a,b,c; de Vernal and Mudie, 1989; de Vernal et al., 1992; Powell, 1992; Williams et al., 1993). Detailed palynostratigraphic studies in the Mediterranean have been made by Habib (1971), Jan du Chêne (1977), Powell (1986a,b,c), Corradini and Biffi (1988), Benzakour (1992), and Versteegh and Zonneveld (1994). First and last appearance datums (FADs and LADs) or acmes of indicator species in these works have been calibrated to the magnetostratigraphy and with nannofossil, planktonic foraminifer, and diatom biochronologies. We have used these data to assign probable ages to the dinocyst ranges for ODP Hole 898A, establishing a provisional zonation. Five provisional dinocyst zones identified in Hole 898A are defined below in ascending stratigraphic order (Fig. 2, Table 1). The age determination based on the dinocysts is compared with the ages determined by the Shipboard Scientific

Table 1. Occurrences of dinocyst and acritarch taxa in lower Miocene to middle Pleistocene sediments in Hole 898A.

Shipboard ages	Pleistocene														
	N23 to N22 (upper)														
Planktonic foraminiferal zones															
Calcareous nannofossil zones	NN21	NN20								NN 19F					
Dinocyst zones	V														
Core, section	1H-1	1H-2	1H-3	1H-4	1H-6	2H-2	2H-3	2H-3	2H-4	2H-4	3H-3	3H-5	4H-2	4H-3	4H-6
Interval (cm)	10-12	65-66	98-100	9-11	3-5	142-144	38-40	98-100	62-64	92-94	57-59	17-19	13-139	19-21	46-48
Dinocyst concentration/ml (×1000)	1.36	0.42	1.16	0.3	2.87	1.18	0.47	1.43	2.21	3.13	1.5	0.7	0.88	0.97	1.6
Pollen concentration/ml (×1000)	0.54	0.06	1.08	0.52	0.47	2.9	1.05	1.8	0.14	1.52	0.04	0.58	0.03	0.08	1.59
D:P	2.5	6.9	1.1	0.5	6.1	0.4	0.4	0.8	15	2.1	37	1.2	28	12	0.91
Sedimentology (turbidite/pelagite)	T	P	P	T	P	T	T	T	P	T	P	T	P	T	P
<i>Nematosphaeropsis labyrinthus</i>	F		R		F			R	R		R				
<i>Impagidinium patulum</i>	R	C	F		F			F	A		R	F			R
<i>Operculodinium centrocarpum</i>	F	F		F	F	F	F	F	F	R	R	F	F	C	F
<i>Tectatodinium pellitum</i>	R		R									R			R
<i>Spiniferites</i> spp. indet.	C	F	C		R	A	A	C	C	C	A	C	A	A	A
<i>Spiniferites mirabilis</i>	F	R			R			F	R	R	R	R			
<i>Achomosphaera andalusiensis</i>	R	R	F	F	A	C	F	F	F	F		R	F	F	F
<i>Bitectatodinium tepikiense</i>	A	A	A	C	F		C	C	F	C	F	A	C	F	A
<i>Operculodinium israelianum/crassum</i>	R	R	R	F	R			F	F						
<i>Impagidinium sphaericum</i>	R	R			R				F	R			R		
<i>Impagidinium aculeatum</i>		F			R		F	R	R	A		F	C	F	F
<i>Brigantidium</i> spp.				A		C	R	F				F			F
<i>Lingulodinium macherophorum</i>					F		R		F						F
<i>Impagidinium striatum</i>					R		R	R							
<i>Habibacysta tectata</i>					R										
<i>Selenopemphix nephroides</i>						R		R							
<i>Spiniferites elongatus</i>							R								
<i>Spiniferites ramosus</i>								R	R	R	F	R			
<i>Stelladinium stellatum</i>								R							
<i>Multispinula minuta</i>														F	
<i>Polysphaeridium zoharyi</i>															R
<i>Multispinula quanta</i>															
<i>Lejeunecysta communis</i>															
<i>Selenopemphix brevispinosa</i>															
<i>Amiculosphaera umbracula</i>															
<i>Invertocysta lacrymosa</i>															
<i>Impagidinium</i> sp. F Wrenn and Kokinos, 1986															
<i>Melitasphaeridium choanophorum</i>															
<i>Operculodinium janduchenei</i>															
<i>Impagidinium japonicum</i>															
<i>Cymatiosphaera invaginata</i>															
<i>Achomosphaera ramulifera</i>															
<i>Spiniferites bentorii</i>															
<i>Filisphaera filifera</i>															
<i>Impagidinium aliferum</i>															
<i>Reticulosphaera actinocoronata</i>															
<i>Sumatradinium hispidum</i>															
<i>Operculodinium eirikianum</i>															

Note: Abundances = rare (R), <3%; few (F), 3%-15%; common (C), 15%-30%; abundant (A), >30%. Dinocyst concentrations include acritarchs, pollen concentrations include terrestrial spores, all concentrations are ×1000. D:P = ratio of marine to terrestrial palynomorphs. The identification of sediment samples as turbiditic or pelagic is from Milkert (this volume).

Party (1994b), in addition to personal communications from biostratigraphers working with other microfossil groups. Because fewer samples were analyzed from Hole 900A in sediments younger than early Miocene, the assemblages are described in ascending stratigraphic order and compared with the dinocyst zones defined in Hole 898A and with the ages determined by the Shipboard Scientific Party (1994c; Table 2).

PALYNOLOGICAL RESULTS FROM HOLE 898A

Palynomorphs were generally abundant and well preserved in Unit I. Dinocyst concentrations in this unit range between 200 and 36,100 cysts/ml (Table 1). Pollen concentrations were generally high

in the upper 13 cores, ranging between 60 and 49,400 grains/ml. In Cores 14 through 18, pollen concentrations are lower, ranging between 130 and 2800 grains/ml. Dinocyst concentrations in Unit II range between 620 and 114,000 cysts/ml. Palynomorph preservation was relatively poor in lithostratigraphic Unit II.

Reworked dinocysts were present in small numbers in many samples, especially in the Pliocene-Pleistocene sequence, although we probably underestimated the degree of reworking, because most taxa present in these samples were long ranging and therefore could not be identified by their stratigraphic discordance. Although an attempt was made by visual inspection (primarily based on sediment color) to avoid processing turbiditic sediments for palynological analysis because they were likely to confuse the production of a chronostratigraphic framework, the majority of samples processed were later

Table 1 (continued).

Shipboard ages	Pleistocene														
Planktonic foraminiferal zones	N23 to N22 (upper)														
Calcareous nannofossil zones	NN 19F							NN 19E							
Dinocyst zones	V			IV				IV							
Core, section	5H-1	5H-2	5H-3	5H-5	5H-7	6H-3	6H-7	7H-3	7H-4	7H-6	8H-1	8H-5	8H-7	9H-6	9H-7
Interval (cm)	33-35	116-118	51-53	87-89	38-40	134-137	15-17	77-79	82-84	110-112	42-44	103-105	58-60	104-107	66-68
Dinocyst concentration/ml (×1000)	11	9.98	0.2	11.1	32.6	4.35	6.95	1.23	10.8	0.92	2.95	0.64	0.16	2.53	9.42
Pollen concentration/ml (×1000)	15.5	8.93	0.12	8.17	49.4	5.75	11.8	1.19	18.1	0.07	1.86	0.22	0.16	1.88	4.48
D:P	0.71	1.1	1.7	1.36	0.66	0.76	0.59	0.83	0.96	12.3	1.6	2.8	1.1	12	2.1
Sedimentology (turbidite/pelagite)	T	P	T	P	T	T	T	D	D	D	?	T	T	P	T
<i>Nematosphaeropsis labyrinthus</i>								R		R					
<i>Impagidinium patulum</i>				R	F	F	R	F	R	F					
<i>Operculodinium centrocarpum</i>	F		R			F		F	F	C		C			F
<i>Tectatodinium pellitum</i>			R								R		R		
<i>Spiniferites</i> spp. indet	C	A	C		F	C	C	F	C	F	C	R	F	F	C
<i>Spiniferites mirabilis</i>						F		R		F	F				R
<i>Achomosphaera andalousiensis</i>			R			R			R	R	F				F
<i>Bitectatodinium tepikiense</i>	F	R	C			F	R	C	R	R	C	R	C	C	C
<i>Operculodinium israelianum/crassum</i>						R				F	C		F		R
<i>Impagidinium sphaericum</i>						R		R		R				R	
<i>Impagidinium aculeatum</i>						F		R		F		A	F	F	
<i>Brigantodinium</i> spp.	A	A	A	A	A	C	A		A	F	C		A		A
<i>Lingulodinium macherophorum</i>		R	R	R		R		F	F	F	F				
<i>Impagidinium striolatum</i>						R									
<i>Habibacysta tectata</i>															
<i>Selenopemphix nephroides</i>			R	R		R	R		R	R	F		F		R
<i>Spiniferites elongatus</i>									R						
<i>Spiniferites ramosus</i>			R			F			R	F	F		F	R	R
<i>Stelladinium stellatum</i>				R	F	R	R		R						
<i>Multispinula minuta</i>	R	R					F						F		F
<i>Polysphaeridium zoharyi</i>										R					
<i>Multispinula quanta</i>		R				R	R		F						
<i>Lejeunecysta communis</i>			R												
<i>Selenopemphix brevispinosa</i>				R											
<i>Amiculospaera umbracula</i>															
<i>Invertocysta lacrymosa</i>															
<i>Impagidinium</i> sp. F Wrenn & Kokinos, 1986															
<i>Melitasphaeridium choanophorum</i>															
<i>Operculodinium janduchenei</i>										R					
<i>Impagidinium japonicum</i>										R					
<i>Cymatospaera invaginata</i>															
<i>Achomosphaera ramulifera</i>										R				R	
<i>Spiniferites bentorii</i>															
<i>Filisphaera filifera</i>														R	
<i>Impagidinium aliferum</i>															
<i>Reticulatosphaera actinocoronata</i>															
<i>Sumatradinium hispidum</i>															
<i>Operculodinium eirikianum</i>															

found to be from turbidites (Milkert, pers. comm., 1994). These are not ideal samples with which to establish chronostratigraphy, but turbidite samples provide insight into the paleoenvironmental conditions conducive to downslope mass wasting processes along the Iberian margin. The pervasive reworking noticed in the palynological preparations is consistent with planktonic foraminifer data that suggest reworking (Shipboard Scientific Party, 1994b).

Dinocyst Stratigraphy

Dinocyst Zone I

Samples 149-898A-28X-2, 58-60 cm through 149-898A-23X-4, 100-103 cm (256.60 through 211.90 mbsf) are early Miocene in age (Table 1, Fig. 2). This zone contains assemblages dominated by *Dapsilodinium* spp., *Homotryblium* spp., and *Apteodinium* spp. The top of this zone is defined by the highest occurrence of *Homotryblium val-*

lum, *Chiropteridium mespilanum*, *Apteodinium spiridoides*, and *Apteodinium?* sp. A of Powell, 1986b. The presence of *Pentadinium laticinctum*, *Homotryblium floripes*, *Hystrichokolpoma cinctum*, *Thalassiphora delicata*, *Impagidinium aspinatum*, and *Caligodinium pynchum* is also consistent with an early Miocene age for sediments in temperate and subtropical regions of the northeast Atlantic (Edwards 1984; Powell 1986a,b). The genera *Pentadinium* and *Thalassiphora* are rare or absent from sediments younger than early middle Miocene (Powell, 1992; Edwards, 1984; Costa and Downie, 1979); *C. pynchum* became extinct at early/middle Miocene boundary (Williams et al., 1993), and *C. mespilanum* and *H. cinctum* persisted until the middle early Miocene in the Mediterranean (Powell, 1986a,b). The last appearance of the genus *Apteodinium* in northwest Europe is in the middle early Miocene (Powell, 1992), and the genus is not reported for sediments younger than early middle Miocene in Italy (Powell, 1986a,b,c). Other notable features are the persistent pres-

Table 1 (continued).

Shipboard ages	Pleistocene													
Planktonic foraminiferal zones	N22 (lower)													
Calcareous nannofossil zones	NN19D							NN19C						
Dinocyst zones	IV													
Core, section	10H-3	10H-5	11H-1	11H-2	11H-4	11H-5	12H-1	12H-3	12H-4	13H-1	13H-6	14H-5	15X-2	15X-4
Interval (cm)	99-101	88-90	111-113	19-21	21-23	148-150	136-139	110-112	70-72	85-87	13-15	1-3	48-50	71-73
Dinocyst concentration/ml (×1000)	4.97	4.34	6.58	5.88	5.25	1.74	6.75	14	10.2	5.57	7.19	6.06	3.5	10.8
Pollen concentration/ml (×1000)	4.97	5.64	3.87	2.1	0.75	4.58	8.33	8.75	11.7	3.71	10.9	0.13	2.19	2.08
D:P	1	0.77	1.7	2.8	7	0.38	0.81	1.6	0.87	1.5	0.66	45	1.6	5.2
Sedimentology (turbidite/pelagite)	P	T	P	P	T/P	T	T	T	T	T	T	T	T	T
<i>Nematosphaeropsis labyrinthus</i>														
<i>Impagidinium patulum</i>	F		F	F		R								
<i>Operculodinium centrocarpum</i>	R			R	F	R	F	R	F		F	F	R	
<i>Tectatodinium pellitum</i>				R										R
<i>Spiniferites</i> spp. indet	F	C	C	F	C		F	F	A	C	R	A	F	F
<i>Spiniferites mirabilis</i>					F				R					F
<i>Achomosphaera andalouisiensis</i>	F	R	F	F	F			R			R	R		
<i>Bitectatodinium tepikiense</i>	C	C	A	A	A	A	F	C	A	F	A	F	F	F
<i>Operculodinium israelianum/crassum</i>		F		R	R	R	C		F		C	C	F	A
<i>Impagidinium sphaericum</i>			F	R		R			R					
<i>Impagidinium aculeatum</i>		R	F	C	F				F					
<i>Brigantedinium</i> spp.	A	A	F			C	A	A	F	A	F	R	C	F
<i>Lingulodinium macherophorum</i>				R	R		F	F			F	C	F	R
<i>Impagidinium strialatum</i>	F				R	C						R		
<i>Habibacysta tectata</i>														
<i>Selenopemphix nephroides</i>	F	R		R			F	F					R	R
<i>Spiniferites elongatus</i>													R	R
<i>Spiniferites ramosus</i>										F			R	
<i>Stelladinium stellatum</i>		R						F						
<i>Multispinula minuta</i>		R		R						F				
<i>Polysphaeridium zoharyi</i>			R				F					R	F	
<i>Multispinula quanta</i>		R					F					R	F	
<i>Lejeunecysta communis</i>							R			R			R	
<i>Selenopemphix brevispinosa</i>														
<i>Amiculosphaera umbracula</i>														
<i>Invertocysta lacrymosa</i>												R	F	
<i>Impagidinium</i> sp. F of Wrenn														
<i>Melitasphaeridium choanophorum</i>														
<i>Operculodinium janduchenei</i>														
<i>Impagidinium japonicum</i>														
<i>Cymatiosphaera invaginata</i>														
<i>Achomosphaera ramulifera</i>														
<i>Spiniferites bentorii</i>														
<i>Filitsphaera filifera</i>														
<i>Impagidinium aliferum</i>														
<i>Reticulatosphaera actinocoronata</i>														
<i>Sumatradinium hispidum</i>														
<i>Operculodinium eirikianum</i>														

ence of *Tuberculodinium vancampoae* and the FAD of *Impagidinium patulum*. This zone probably corresponds to the late Oligocene-early Miocene *Tuberculodinium vancampoae* Interval Biozone of Powell (1992), although the presence of well preserved specimens of the middle Miocene markers *Incertae sedis* I of Edwards, 1984 and *Aptedinium australiense* (G.L. Williams, pers. comm., 1995) is puzzling.

Dinocyst Zone II

Samples 149-898A-22X-4, 111-113 cm through 149-898A- 18X-5, 60-62 cm (202.33-163.7 mbsf) are middle Miocene in age. *Dapsilidinium* spp. are present throughout this zone, together with *Hys-trichosphaeropsis obscura* and *Hystrichokolpoma denticulata*, which are notable species of middle to late Miocene age in the eastern North Atlantic (Powell, 1992). Taxa that are common in upper Pliocene

through Holocene sediments of the Mediterranean, such as *Operculodinium israelianum*, *Operculodinium crassum*, and *Lingulodinium macherophorum*, become dominant within this zone, at the base of Core 18. Dinocyst Zone II is defined by lowest occurrences (LO) of *Achomosphaera andalouisiensis*, *Invertocysta lacrymosa*, and *Impagidinium aculeatum*, which also mark the middle Miocene *Achomosphaera andalouisiensis* Zone of Powell (1992). *Habibacysta tectata* first occurs in Core 18; this species has a middle Miocene through earliest Pleistocene range according to Head (1994a). Rare specimens of the middle Miocene marker *Labyrinthodinium truncatum* are also present, but these are not well preserved and could be reworked. The zone contains the highest occurrences, in Sample 149-898A-22X-4, 113-115 cm, of two species, *Dapsilidinium pseudocol-ligerum* and *Nematosphaeropsis major*, with early late Miocene LAD's (Head et al., 1989a).

Table 1 (continued).

Shipboard ages	Pleistocene			late Pliocene					middle Miocene			early Miocene		
Planktonic foraminiferal zones	N22 (lower)													
Calcareous nannofossil zones	NN19B			NN18					NN7	NN6	NN4		NN1	
Dinocyst zones	IV			III					II			I		
Core, section	16X-1	16X-4	17X-1	17X-2	17X-3	17X-5	17X-6	18X-4	18X-5	18X-CC	22X-4	23X-4	25X-2	28X-2
Interval (cm)	57-59	111-113	92-93	141-143	134-136	130-132	36-39	63-66	60-63	13-16	113-115	100-103	74-76	58-60
Dinocyst concentration/ml (×1000)	5.47	36.1	5.32	9.06	3.58	4.6	2.8	5.44	0.62	114	1.9	1.7	2.1	2.4
Pollen concentration/ml (×1000)	2.74	0.55	2.8	0.62	0.61	0.51	0.8	0.9	0.02	10	0.54	0.85	0.17	0.11
D:P	2	65	1.9	14.6	5.9	9	3.5	4.9	35	11.4	3.5	2	12.5	22
Sedimentology (turbidite/pelagite)	T	P	T	T	T	T	T	P	P	P	P	P	P	P
<i>Nematosphaeropsis labyrinthus</i>								R						R
<i>Impagidinium patulum</i>					R			R					R	
<i>Operculodinium centrocarpum</i>	R			F			F	R				R		R
<i>Tectatodinium pellitum</i>	R			R	R		R	R						R
<i>Spiniferites</i> spp. indet	R	C	C	R	C		C	F	R	R	F			
<i>Spiniferites mirabilis</i>				R	F		R	R						
<i>Achomosphaera andalousiensis</i>				R	R	R	F	R	R	R				
<i>Bitetatodinium tepikiense</i>	F	F	A	R	R			R	R	R				
<i>Operculodinium israelianum/crassum</i>	A	A	C	C	A	A	A	F	F	F				
<i>Impagidinium sphaericum</i>				R										
<i>Impagidinium aculeatum</i>	R			F	R		F	F						
<i>Brigantidium</i> spp.	C		R		R	R	R					C		
<i>Lingulodinium macherophorum</i>	F	F	C	A	F		F	A	A	C	R			R
<i>Impagidinium striolatum</i>	R							R						
<i>Habibacysta tectata</i>		R	R		F	R								
<i>Selenopemphix nephroides</i>								R	R					
<i>Spiniferites elongatus</i>						F		R						
<i>Spiniferites ramosus</i>				R			F	F	R	R	R	R	R	F
<i>Stelladinium stellatum</i>	R													
<i>Multispinula minuta</i>	R				F			R						
<i>Polysphaeridium zoharyi</i>		R	R	R	R			R				F	R	R
<i>Multispinula quanta</i>	R													
<i>Lejeunecysta communis</i>	R				R		R							
<i>Selenopemphix brevispinosa</i>		R												
<i>Amiculosphaera umbracula</i>			R					F	R	F	R	R		
<i>Invertocysta lacrymosa</i>					R	R		R						
<i>Impagidinium</i> sp. F of Wrenn		R					R							
<i>Melitasphaeridium choanophorum</i>	R		R											
<i>Operculodinium janduchenei</i>	R	R											R	
<i>Impagidinium japonicum</i>				R										
<i>Cymatiosphaera invaginata</i>				R			R	R	R					
<i>Achomosphaera ramulifera</i>	R	R		R										
<i>Spiniferites bentorii</i>	R													
<i>Filisphaera filifera</i>				R				R		R				
<i>Impagidinium aliferum</i>				R			R					R		
<i>Reticulosphaera actinocoronata</i>				R							R		R	F
<i>Sumatradinium hispidum</i>				R			R	R						
<i>Operculodinium eirikianum</i>				R			F	F	F	F				

Dinocyst Zone III

Samples 149-898A-18X-4, 63-65 cm through 149-898A-17X-2, 141-143 cm (162.25-150.41 mbsf) are assigned a late Pliocene age, although the age of samples from Core 18 are uncertain because of the lack of marker nannofossils (Liu and Maiorano, this volume; Gervais, this volume). This zone contains assemblages dominated by *Operculodinium israelianum/O. crassum* and *Lingulodinium macherophorum*. The late Pliocene age is supported by the acme of *Impagidinium bacatum* and the highest occurrences of *Operculodinium? eirikianum*, *Impagidinium aliferum* and *Cymatiosphaera invaginata*, which have their highest occurrences in uppermost Pliocene to lowest Pleistocene sediments of the North Atlantic (Head et al., 1989a; Mudie 1987). The zone also contains the lowest occurrences of *Impagidinium* sp. F of Wrenn and Kokinos, 1986 and *Filisphaera filifera* which have FADs in the early Pliocene of the North Atlantic;

the latter is also common in late Pliocene sediments in the British Isles (Head, 1993). The occurrence of the Miocene marker *Sumatradinium hispidum*, however, suggests reworking.

Dinocyst Zone IV

Samples 149-898A-17X-1, 92-93 cm through 149-898A-5H-3, 51-53 cm (148.43-41.21 mbsf) are early Pleistocene in age, as supported by the LAD in Sample 149-898A-14H-5, 1-3 cm of *Amiculosphaera umbracula*, which became extinct in the early Pleistocene in the Mediterranean (Powell, 1989c), and in Sample 149-898A-5H-3, 51-53 cm of *Lejeunecysta communis*, which became extinct in the early Pleistocene (Harland, 1992). Protoperidinioids first become common in Sample 149-898A-16X-1, 57-59 cm, with diverse *Brigantidium* spp., and rare *Stelladinium stellatum*, *Selenopemphix nephroides*, *Multispinula quanta* and *Multispinula? minuta* (= *Algi-*

Table 1 (continued).

Shipboard ages	Pleistocene													
Planktonic foraminiferal zones	N22 (lower)													
Calcareous nannofossil zones	NN19D							NN19C						
Dinocyst zones	IV													
Core, section	10H-3	10H-5	11H-1	11H-2	11H-4	11H-5	12H-1	12H-3	12H-4	13H-1	13H-6	14H-5	15X-2	15X-4
Interval (cm)	99-101	88-90	111-113	19-21	21-23	148-150	136-139	110-112	70-72	85-87	13-15	1-3	48-50	71-73
Dinocyst concentration/ml (×1000)	4.97	4.34	6.58	5.88	5.25	1.74	6.75	14	10.2	5.57	7.19	6.06	3.5	10.8
Pollen concentration/ml (×1000)	4.97	5.64	3.87	2.1	0.75	4.58	8.33	8.75	11.7	3.71	10.9	0.13	2.19	2.08
D:P	1	0.77	1.7	2.8	7	0.38	0.81	1.6	0.87	1.5	0.66	45	1.6	5.2
Sedimentology (turbidite/pelagite)	P	T	P	P	T/P	T	T	T	T	T	T	T	T	T
<i>Galeacysta etrusca</i>														
<i>Operculodinium psilatam</i>														
<i>Tuberculodinium vancampoeae</i>														
<i>Hystriocholpoma rigaudiae</i>														
<i>Hystriochosphaeropsis obscura</i>														
<i>Spiniferites rubinus</i>														
<i>Impagidinium? pallidum</i>														
<i>Nematosphaeropsis oblonga</i>														
<i>Hystriocholpoma denticulata</i>														
<i>Impagidinium bacatum</i>														
<i>Dapsilidinium</i> sp. Wrenn & Kokinos, 1986														
<i>Spiniferites membranaceus</i>														
<i>Habibacysta tectata</i>														
<i>Nematosphaeropsis major</i>														
<i>Impagidinium velorum</i>														
<i>Micrhystridium</i> sp.														
<i>Dapsilidinium pseudocolligerum</i>														
<i>Homotryblium vallum</i>														
<i>Polysphaeridium congregatum</i>														
<i>Polysphaeridium congregatum</i>														
<i>Homotryblium floripes</i>														
<i>Apteodinium</i> sp. A of Powell 1986														
<i>Cyclopsiella granosa</i>														
<i>Chiropteridium mespilanum</i>														
<i>Dapsilidinium pastielsii</i>														
<i>Caligodinium pynchum</i>														
<i>Incertae sedis</i> I Edwards 1984														
<i>Apteodinium australiense</i>														
<i>Apteodinium spiridoides</i>														
<i>Palaeocystodinium golzowense</i>														
<i>Batiacasphaera sphaerica</i>														
<i>Homotryblium tenuispinosum</i>														
<i>Thalassiphora delicata</i>														
<i>Pentadinium laticinctum</i>														
<i>Thalassiphora pelagica</i>														
<i>Thalassiphora</i> cf. <i>Th. pansa</i>														
<i>Distatodinium paradoxum</i>														
<i>Impagidinium aspinatum</i>														
<i>Cannosphaeropsis</i> cf. <i>C. utinensis</i>														
<i>Hystriocholpoma cinctum</i>														

dasphaeridium? minuta). Common gonyaulacoid dinocyst taxa in early Pleistocene sediments include *Bitectatodinium tepikiense*, *Operculodinium centrocarpum*, and various *Spiniferites* spp., with occasional peaks of *Impagidinium* spp.

Dinocyst Zone V

Samples 149-898A-5H-2, 116-118 cm through 149-898A-1H-1, 10-12 cm are assigned to the middle Pleistocene based on the abundance of *Achomosphaera andalouensis* which has its LAD in the late Pleistocene in the northwest Atlantic (de Vernal and Mudie, 1989; Mudie, 1992). *Brigantedinium* spp., *Bitectatodinium tepikiense*, various *Spiniferites* spp. and *Impagidinium* spp., especially *I. patulum*, dominate the assemblages. Persistent presence of *Nematosphaeropsis labyrinthus* is also characteristic of this zone.

Paleoenvironmental Interpretation, Hole 898A

Little is known about the environmental conditions that prevailed during the early Miocene, because most of the dinocyst taxa present in Dinocyst Zone I are extinct. The presence of the extant tropical dinocyst *Tuberculodinium vancampoeae* (Harland, 1983; Edwards et al., 1991), however, suggests warmer surface water conditions than prevail at present above the Iberia Abyssal Plain.

Surprisingly consistent dinocyst assemblages are found from Sample 149-898A-18X-CC, 13-16 cm (middle Miocene, NN6) through Sample 149-898A-14H-5, 1-3 cm (early Pleistocene, NN19C) in Hole 898A, suggesting the existence of uniform oceanographic conditions through much of the late Cenozoic. This interval comprises lithostratigraphic Unit IIA and the lower 35 meters of Unit I. *Tuberculodinium vancampoeae*, *Impagidinium aculeatum*, and

Table 1 (continued).

Shipboard ages	late Pliocene							middle Miocene			early Miocene			
Planktonic foraminiferal zones	N22 (lower)							N14	N13	N7	N6	N5	N4	
Calcareous nannofossil zones	NN19B		NN18					NN7	NN6		NN4		NN1	
Dinocyst zones	IV			III				II			I			
Core, section	16X-1	16X-4	17X-1	17X-2	17X-3	17X-5	17X-6	18X-4	18X-5	18X-CC	22X-4	23X-4	25X-2	28X-2
Interval (cm)	57-59	111-113	92-93	141-143	134-136	130-132	36-39	63-66	60-63	13-16	113-115	100-103	74-76	58-60
Dinocyst concentration/ml (×1000)	5.47	36.1	5.32	9.06	3.58	4.6	2.8	5.44	0.62	114	1.9	1.7	2.1	2.4
Pollen concentration/ml (×1000)	2.74	0.55	2.8	0.62	0.61	0.51	0.8	0.9	0.02	10	0.54	0.85	0.17	0.11
D:P	2	65	1.9	14.6	5.9	9	3.5	4.9	35	11.4	3.5	2	12.5	22
Sedimentology (turbidite/pelagite)	T	P	T	T	T	T	T	P	P	P	P	P	P	P
<i>Galeacysta etrusca</i>				R										
<i>Operculodinium psilatam</i>				R				R						
<i>Tuberculodinium vancampoae</i>				R				R				R	R	
<i>Hystrichokolpoma rigaudiae</i>					R									R
<i>Hystrichosphaeropsis obscura</i>					R			R	R	R	F			
<i>Spiniferites rubinus</i>					R							R		
<i>Impagidinium? pallidum</i>								R			R	R	R	R
<i>Nematosphaeropsis oblonga</i>								R						
<i>Hystrichokolpoma denticulata</i>								R		R				
<i>Impagidinium bacatum</i>								R						
<i>Dapsilidinium</i> sp. Wrenn & Kokinos, 1986									R	C		R	A	
<i>Spiniferites membranaceus</i>										F				R
<i>Habibacysta tectata</i>					R			R		R				
<i>Nematosphaeropsis major</i>											R	R		
<i>Impagidinium velorum</i>											R	F	R	R
<i>Michrystidium</i> sp.											R	A		
<i>Dapsilidinium pseudocolligerum</i>											R	R		R
<i>Homotryblium vallum</i>												R		
<i>Polysphaeridium congregatum</i>												R		
<i>Polysphaeridium congregatum</i>												R		
<i>Homotryblium floripes</i>												R	C	F
<i>Apteodinium</i> sp. A of Powell 1986												F	R	
<i>Cyclopsiella granosa</i>												R	R	R
<i>Chiropteridium mespilanum</i>												R	R	F
<i>Dapsilidinium pastielsii</i>												C	A	R
<i>Caligodinium pynchum</i>												R	F	R
<i>Incertae sedis</i> I Edwards 1984												R	R	R
<i>Apteodinium australiense</i>												R	F	R
<i>Apteodinium spiridoides</i>												R	R	F
<i>Palaeocystodinium golzowense</i>													R	
<i>Batiacasphaera sphaerica</i>													R	
<i>Homotryblium tenuispinosum</i>												R		
<i>Thalassiphora delicata</i>													R	R
<i>Pentadinium laticinctum</i>													R	F
<i>Thalassiphora pelagica</i>														R
<i>Thalassiphora</i> cf. <i>Th. pansa</i>														R
<i>Distatodinium paradoxum</i>														R
<i>Impagidinium aspinatum</i>														R
<i>Cannosphaeropsis</i> cf. <i>C. utinensis</i>														R
<i>Hystrichokolpoma cinctum</i>														R

Polysphaeridium zoharyi are present in these sediments, but *Lingulodinium machaerophorum* and *Operculodinium israelianum/O. crassum* appear to have dominated dinocyst assemblages over an 11 m.y. interval. This microflora records subtropical to temperate conditions (Mudie, 1992; Edwards et al., 1991; Versteegh and Zonneveld, 1994), and a strong inner neritic environmental influence is suggested by *L. machaerophorum* and *O. israelianum* (Harland, 1983; Versteegh and Zonneveld, 1994). The dominance of taxa that currently characterize neritic environments indicates transport of these cysts onto the abyssal plain. This transport, and the high dinocyst concentrations below low productivity subtropical surface waters, may result from downslope mass wasting from the Iberia Margin; alternatively, these cysts, which are common in Quaternary sequences from the Mediterranean (Aksu et al., 1995), may have been transported in Mediterranean overflow water at intermediate depths.

The lowest abundant occurrence, in Sample 149-898A-17X-1, 92-93 cm, of *Bitectatodinium tepikiense*, which is common in the subpolar eastern North Atlantic (Harland, 1983; Mudie, 1992), indicates cooling of surface waters at the beginning of the Pleistocene at Site 898, although *Operculodinium israelianum/O. crassum* and *Lingulodinium machaerophorum* remain common to abundant. The lowest occurrence of high percentages of protoperidinioid cysts, including the lowest common occurrence of *Brigantedinium* spp., is in Sample 149-898A-16X-1, 57-59 cm, and over the overlying 10 m, high percentages of protoperidinioid cysts, especially *Brigantedinium simplex*, alternate with high percentages of *Operculodinium israelianum/O. crassum* and *Lingulodinium machaerophorum*.

The disappearance of the *Lingulodinium machaerophorum-Operculodinium israelianum/O. crassum* microflora between Samples 149-898A-14H-5, 1-3 cm and 149-898A-13H-6, 13-15 cm (129.23-

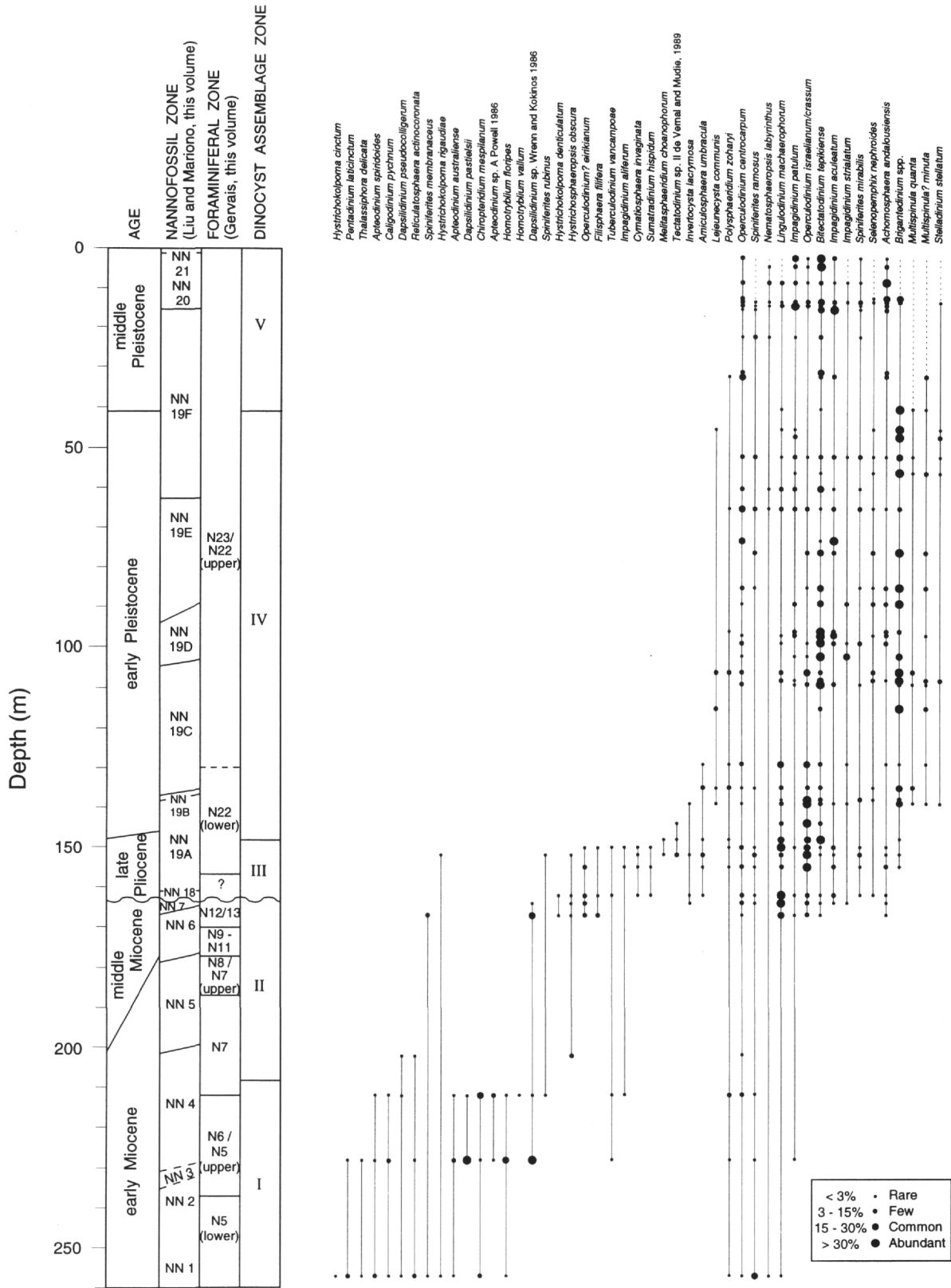


Figure 2. Range chart for selected dinoflagellate cysts and acritarchs in early Miocene to middle Pleistocene sediments in Hole 898A and a suggested revised chronostratigraphy based on defined dinocyst zones. Also shown are planktonic foraminiferal zones (from Gervais, this volume) and calcareous nannofossil zones (from Shipboard Scientific Party, 1994b, and Liu and Mariono, this volume).

Table 2. Ranges of dinocyst and acritarch taxa in lower Miocene to upper Pleistocene sediments in Hole 900, informal dinocyst assemblages described from these sediments, and chronostratigraphic zonation.*

Shipboard age assignment**	Pleistocene					late Pliocene		early Plio.	late Miocene			mid Mio.	early Miocene			
	6		5		4		3	2		1						
Dinocyst assemblages	1H-1	3H-1	4H-1	6H-4	9H-2	10R-2	10R-4	11R-4	12R-4	14R-5	16R-5	17R-3	18R-2	21R-1	30R-4	36R-3
Core, section	28-30	11-13	110-112	67-69	23-25	99-101	31-33	100-102	18-20	148-150	81-83	10-12	58-60	101-103	91-93	95-97
Interval (cm)																
Dinocyst concentration/ml	490	2754	3198	3617	697	97	267	14	110	48	23	169	105	98	197	115
Pollen concentration/ml	42	334	571	0	4	0	13	0	8	1	2	4	5	3	3	2
D:P	11.7	8.25	5.6	—	174	—	20.5	—	13.8	48	11.5	42.3	21	32.7	65.7	57.5
<i>Impagidinium striatum</i>	F		R													
<i>Brigantedinium</i> spp.	R						R									
<i>Nematosphaeropsis labyrinthus</i>	R		R	R			R				F			R		
<i>Operculodinium centrocarpum</i>	F	C		F	F	R	F				R	R				
<i>Spiniferites</i> spp.	F	C	C	F	R	R	F		F	C	F	C				
<i>Spiniferites ramosus</i>	R	F	R			F	F				F			C	R	
<i>Achomosphaera andalousiensis</i>	F				F								F			
<i>Bitectatodinium tepikiense</i>	C	C														
<i>Impagidinium aculeatum</i>																
<i>Impagidinium</i> sp.	R		R	R		F	C									
<i>Impagidinium aculeatum</i>	F	F	A	F	C	F	C	P	R				R			
<i>Lingulodinium machaerophorum</i>	F			F	F	C	R			C	F	F	F		R	
<i>Spiniferites mirabilis</i>		R		R		R							R			
<i>Impagidinium patulum</i>			R		F	F	R	P	A			R		R		
<i>Polysphaeridium zoharyi</i>				R						C	R	F	F	R	R	C
<i>Operculodinium israelianum</i>				A	F	C	F				F	F	R			
<i>Operculodinium crassum</i>					F	C	R						A			
<i>Multispinula quanta</i>					R											
<i>Stelladinium stellatum</i>					R											
<i>Amiculosphaera umbracula</i>					F			R								
<i>Melitasphaeridium choanophorum</i>					R							R				
<i>Impagidinium sphaericum</i>						F	R									
<i>Impagidinium</i> sp. A of Mudie, 1987						F	R									
<i>Impagidinium aliferum</i>						R	R									
<i>Micrhystridium</i> sp.						R	R					R				
<i>Cymatosphaera invaginata</i>							F						R			
<i>Spiniferites belearius</i>							F									
<i>Invertocysta lacrymosa</i>							F									
<i>Invertocysta tabulata</i>							F									
<i>Galeacysta etrusca</i>							R									
<i>Impagidinium bacatum</i>							R									
<i>Operculodinium? eirikianum</i>							R									
<i>Operculodinium janduchenei</i>							R				R	F				
<i>Reticulosphaera actinocoronata</i>											F					
<i>Homotryblum floripes</i>														R	F	C
<i>Corrudinium harlandii</i>																
<i>Pyxidiella? simplex</i>																
<i>Spiniferites rubinus</i>																
<i>Sumatradinium druggii</i>																
<i>Selenopemphix nephroides</i>																
<i>Impagidinium</i> sp. F. of Wrenn and Kokinos, 1986																
<i>Batiacasphaera micropapillata</i> complex																
<i>Labyrinthodinium truncatum</i>																
<i>Nematosphaeropsis major</i>																
<i>Impagidinium velorum</i>																
<i>Hystriochosphaeropsis obscura</i>																
<i>Spiniferites membranaceus</i>														R		
<i>Achomosphaera ramulifera</i>																
<i>Apteodinium spiridoides</i>																R
<i>Apteodinium australiense</i>														R	R	R
<i>Chiropteridium mespilanum</i>														F	R	R
<i>Dapsilidinium pseudocolligerum</i>														C	C	C
<i>Cannosphaeropsis</i> cf. <i>C. utinensis</i>														R	R	R
<i>Pentadinium laticinctum</i>														R	R	R
<i>Dapsilidinium pastielsii</i>														R	F	
<i>Caligodinium pycnum</i>															R	R
<i>Tuberculodinium vancampoeae</i>															R	R
<i>Homotryblum oceanicum</i>															F	C
<i>Homotryblum tenuispinosum</i>															F	C
<i>Cyclopsiella granosa</i>															F	F
<i>Hystriocholpoma cinctum</i>															F	F
<i>Polysphaeridium congregatum</i>															R	R
<i>Hystriocholpoma rigaudiae</i>															R	R
<i>Thalassiphora pelagica</i>															F	F
<i>Apteodinium</i> sp. A of Powell, 1986a															R	R
<i>Thalassiphora delicata</i>															R	R
Incertae sedis I of Edwards, 1984															R	R
<i>Polysphaeridium subtile</i>															R	R
<i>Homotryblum vallum</i>															F	F
<i>Distatodinium paradoxum</i>															R	R

Notes: *Shipboard Scientific Party (1994b), **Shipboard Scientific Party (1994c). Dinocyst concentrations include acritarchs; pollen concentrations include terrestrial spores. Abundances = rare (R), <3%; few (F), 3%-15%; common (C), 15%-30%; abundant (A), >30%; P = cysts in very sparse samples. D:P = ratio of marine to terrestrial palynomorphs.

121.33 mbsf) records a major paleoceanographic change during the early Pleistocene. The upper 13 cores (or 123.2 m) of Hole 898A are generally characterized by high percentages of *Bitectatodinium tepikiense*, *Spiniferites* spp., and *Operculodinium centrocarpum*, an assemblage similar to the slope ecofacies of Edwards et al. (1991) and Mudie (1992). These temperate taxa record substantially lower sea surface temperatures than had apparently existed since the middle Miocene. Calcareous nannofossil data provide an age of approximately 1.4 Ma for this oceanographic change, as it occurs between the highest occurrence of *Calcidiscus macintyreii*, >10 μ m (1.47 Ma) in Sample 149-898A-15X-CC, and the lowest occurrence of *Gephyrocapsa caribbeanica* >5.5 μ m (1.37 Ma) in Sample 140-898A-13H-4, 134 cm (Shipboard Scientific Party, 1994b). A similar water mass transition around 1.4 Ma is recorded on the New Jersey Margin (McCarthy, 1992), suggesting a climatically-forced mechanism affecting the subtropical gyre. There is evidence for the existence of a high velocity phase of the Gulf Stream over the past 1.5 m.y., accompanying climatic cooling (Kaneps, 1979).

The last 1.4 m.y. have been marked by alternating peaks of *Brigantedinium* spp. (dominantly *B. simplex*), and of *Impagidinium* spp. overprinting the *Bitectatodinium tepikiense*-*Spiniferites* spp.-*Operculodinium centrocarpum* microflora. The presence of cysts of *Brigantedinium* in Hole 898A is almost invariably associated with low D:P ratios (Table 1), which is a strong indication that these cysts are transported onto the abyssal plain together with terrigenous material. This may reflect increased turbidite activity during glacioeustatic sea-level lowstands (Miller et al., 1987), or possibly meltwater plumes transporting large terrigenous loads with included pollen content. Either of these interpretations is consistent with the higher proportion of sand and silt in the upper 12 cores compared to those below (Shipboard Scientific Party, 1994b). The good correlation between sedimentological identification of turbidites (Milkert, pers. comm., 1994), low D:P ratios and the presence of *Brigantedinium* cysts indicates that, on the Iberia Abyssal Plain, the palynological criteria can be used as an index of turbidite deposition in deep sea sediments. Sediments described by Milkert as pelagites usually have high D:P ratios and often have common to abundant *Impagidinium* cysts. The genus *Impagidinium* characterizes oceanic environments (Wall et al., 1977; Harland, 1983) and abundance of this genus suggests pelagic influx of cysts from the subtropical gyre with minimal influx from neritic environments, possibly during glacioeustatic sea level highstands.

Achomosphaera andalousiensis, *Nematosphaeropsis labyrinthus*, and *Impagidinium patulum* become more abundant in the middle Pleistocene, though *Bitectatodinium tepikiense*, *Spiniferites* spp. and *Operculodinium centrocarpum* remain common. Except for the extinct *Achomosphaera andalousiensis*, this assemblage is similar to the modern assemblage in the NAC (Harland, 1983). The absence of late Pleistocene sediments in Hole 898A may be related to the paleoceanographic change recorded by this change in microflora.

PALYNOLOGICAL RESULTS FROM HOLE 900A

Palynomorphs are generally less abundant and diverse in Hole 900A than in Hole 898A. Dinocyst concentrations are low, ranging from zero to 3617 cysts/ml. Pollen concentrations are very low, with several samples barren of terrestrial palynomorphs, and others ranging from 1 to 571 grains/ml. Dinocyst preservation was often moderately poor to very poor in the calcareous pelagic sediments of Unit II, with many specimens being strongly oxidized or mechanically damaged (folded or torn). Poor preservation has also been reported in pelagic sediments from the Rockall Plateau in the eastern North Atlantic (Edwards, 1984; Harland, 1989).

Dinocyst Assemblages

Because few samples from Hole 900A younger than early Miocene in age were analyzed, biostratigraphic zones were not established for this hole. Instead, the assemblages are described in ascending stratigraphic order and compared with the dinocyst zones defined in Hole 898A and with the ages determined by the Shipboard Scientific Party (1994c; Table 2).

Dinocyst Assemblage 1

Samples 149-900A-36R-3, 94-96 cm through 149-900A-21R-1, 101-103 cm (328.86 through 181.31 mbsf) are early Miocene in age and correspond to Dinocyst Zone I of Hole 898A. Assemblages are dominated by *Dapsilidinium* spp. (especially *D. pseudocolligerum*), and the LADs of *Chiropteridium mespilanum*, and *Apteodinium spiridoides* in Sample 149-900A-21R-1, 101-103 cm are consistent with the early Miocene age assigned to Dinocyst Zone I in Hole 898A. The presence of *Hystrichokolpoma cinctum*, *Distatodinium paradoxum*, *Homotryblium vallum*, *Thalassiphora pelagica*, *Thalassiphora delicata*, *Dapsilidinium pastielsii*, *Apteodinium australiense*, and *Pentadinium laticinctum* is also similar to the lower Miocene sequence in Hole 898A. In general, however, there is a lower abundance of cysts in the early Miocene interval in Hole 900A.

Dinocyst Assemblage 2

Samples 149-900A-18R-2, 58-60 cm through 149-900A-14R-5, 148-150 cm (153.9 through 120.19 mbsf) have a middle through early late Miocene age (Shipboard Party, 1994a). The assemblage is characterized by the acme of *Operculodinium crassum*, together with common occurrences of *Operculodinium? eirikianum*, *Operculodinium israelianum*, *Polysphaeridium zoharyi* and *Lingulodinium machaerophorum*; Sample 149-900A-15R-4, 114-116 cm is barren of dinocysts. The FADs of *Achomosphaera andalousiensis* and *Impagidinium aculeatum* in Sample 149-900A-18R-2, 58-60 cm and the presence of *Labyrinthodinium truncatum* supports a middle Miocene age for this sample (Powell, 1992). Calcareous nannofossils also indicate a middle Miocene age for Sample 149-900A-18R-2, 58-60 cm, but Samples 149-900A-17R-3, 10-12 cm and 149-900A-16R-5, 81-83 cm were assigned to the late Miocene zone NN11A. This age is supported by the lowest occurrence of *Operculodinium janduchenei* in Samples 149-900A-17R-3, 10-12 cm and 149-900A-16R-6, 81-83 cm; this species has a lower upper Miocene through Pliocene age range in the North Atlantic (Head et al., 1989a). In general, however, the dinocyst assemblages in Hole 900A are similar to the middle Miocene assemblages at the top of Dinocyst Zone II in Hole 898A, and no other distinctive late Miocene markers were found.

Dinocyst Assemblage 3

Samples 149-900-12R-4, 18-20 cm through 149-900A-11R-4, 100-102 cm (98.9 through 89.22 mbsf), which have a late Miocene to early Pliocene age, are characterized by very low species diversity, with assemblages strongly dominated by *Impagidinium aculeatum*, *Impagidinium patulum*, and *Spiniferites mirabilis/hyperacanthus*. Similar assemblages are reported for earliest Pliocene assemblages in the central Mediterranean (Benzakour, 1992). Sediments of late Miocene to early Pliocene age were absent in Hole 898A.

Dinocyst Assemblage 4

Samples 149-900A-10R-4, 31-33 cm and 149-900A-10R-2, 99-101 cm (80.43-78.1 mbsf) are assigned a late Pliocene shipboard age

which is supported by the LADs of *Impagidinium aliferum*, *Invertocysta lacrymosa*, and by the acme of the acritarch *Cymatiosphaera invaginata*, as found at DSDP Site 607 in the subtropical N. Atlantic (Mudie, 1987). *Lingulodinium machaerophorum* dominates the assemblages, together with *Operculodinium crassum* and *Operculodinium israelianum*, as found in Dinocyst Zone III in Hole 898A and in the Mediterranean Pliocene (Benzakour, 1992). Early Pliocene assemblages in Hole 900A differ from Dinocyst Zone III in Hole 898A in the sparsity of *Operculodinium? eirikianum* and protoperidinioids, and the greater diversity and abundance of *Impagidinium* species, including *Impagidinium* sp. A. of Mudie, 1987.

Dinocyst Assemblage 5

Sample 149-900A-9R-2, 23-25 cm (66.23-66.25 mbsf) was assigned a late Pliocene age by the Shipboard Scientific Party (1994c), but the dinocyst assemblage is very similar to that found in Sample 149-900A-6R-4, 68-70 cm (46.68-46.70 mbsf), assigned to the early Pleistocene. *Lingulodinium machaerophorum*, *Operculodinium crassum* and *Operculodinium israelianum* are dominant in both samples. The highest occurrence of *Ambicosphaera umbracula* and *Melittasphaeridium choanophorum* in Sample 149-900A-9R-2, 23-25 cm is consistent with a late Pliocene age, as recorded at most sites in the North Atlantic (Mudie et al., 1990); however, it does not negate an early Pleistocene age, as questionably proposed by de Vernal (1992) for *A. umbracula*. This assemblage corresponds to the lower part of Dinocyst Zone IV (i.e., pre-~1.4 Ma) defined in Hole 898A.

Dinocyst Assemblage 6

Samples 149-900A-4R-1, 111-113 cm to 149-900A-1R-1, 29-31 cm (20.93-0.29 mbsf) are assigned to the Pleistocene, corresponding to upper Dinocyst Zone IV and Dinocyst Zone V defined in Hole 898A, with the main difference being the much higher G:P and D:P ratios in Hole 900A. The upper 4 cores in Hole 900A are rich in *Impagidinium aculeatum*, *Spiniferites* spp. (mainly *S. mirabilis* and *S. delicatus*), *Bitectatodinium tepikiense*, and *Operculodinium centrocarpum*.

Paleoenvironmental Interpretation, Hole 900A

Dinoflagellate assemblages record similar paleoenvironmental conditions at Sites 898 and Site 900. Beginning in the middle Miocene, the *Lingulodinium machaerophorum*-*Operculodinium israelianum*/*O. crassum* assemblage recorded in Hole 898A can also be identified in Hole 900A, despite the relatively lower diversity and lower productivity and/or poorer preservation in Hole 900A. The better recovery of late Miocene to late Pliocene sediments in Hole 900A, however, shows that this microflora did not persist continuously over 11 m.y., as was assumed from the incomplete stratigraphy in Hole 898A. At Site 900, sediments deposited in the late Miocene through earliest Pliocene (Zone NN11 b to lower zone NN12; Shipboard Scientific Party, 1994c) are characterized by sparse, very low-diversity gonyaulacoid dinocyst assemblages. This suggests blooms of autotrophic dinoflagellates in low-productivity, warm, surface waters. The *Impagidinium*-dominated assemblage in Samples 149-900 A-12R-4, 18-20 cm and 149-900A-11R-4, 100-102 cm suggests the existence, at Site 900 during the late Miocene, of conditions such as those presently characterizing the subtropical gyre. This would suggest that the "Mediterranean" cysts, *Lingulodinium machaerophorum* and *Operculodinium israelianum*/*O. crassum*, were transported onto the Iberia Abyssal Plain in the Mediterranean overflow, but that this was cut off during this interval when the outflow of Mediterranean water was prevented by shallowing or closure of the straits between Iberia and North Africa (e.g., as described by Cita, 1979). The dominance of *Impagidinium* spp. over this interval also supports the

contention that *Impagidinium* cysts dominate oceanic sediments primarily because of the absence of other cysts (cf. Zonneveld, 1995).

The high ratios of marine vs. terrestrial palynomorphs (D:P; Table 2) record low terrigenous influx throughout the Miocene to Pleistocene, in contrast to the sequence at Site 898 where late Pliocene-Pleistocene turbidite sediments, especially those deposited in the last ~1.4 m.y., are almost invariably associated with low D:P. In addition, protoperidinioid dinocyst taxa are common to abundant through most of the Pleistocene sequence in Hole 898A (except during peak interglacials), whereas there are very few protoperidinioid cysts in Hole 900A. The gonyaulacoid component of the Pleistocene samples in Hole 898A, however, resembles the dinocyst assemblage in Hole 900A. It is possible that the small number of samples analyzed from Hole 900A resulted in the random sampling of only interglacial sediments for analysis, because interglacial sediments in Hole 898A contained very few protoperidinioid cysts. The relative scarcity of terrigenous siliciclastic sediments, the very high D:P, and the very low number of protoperidinioid dinocysts in these sediments is difficult to explain, given the location of Site 900 at the base of the continental rise, 43 km closer to the continent than Site 898. An explanation for the low terrigenous influx at this site is that the high velocity of mud-dominated turbidity flows would have kept most of the sand content in turbulent suspension, bypassing the continental rise to be deposited on the abyssal plain (Shipboard Scientific Party, 1994c). The very low numbers of pollen and protoperidinioid dinocysts in Hole 900A appears to support this theory, since a large percentage of these may be transported to the abyssal plain from neritic environments via turbidity flows.

CONCLUSIONS

Dinocyst assemblages identified from Holes 898A and 900A give ages which are generally in agreement with those based on calcareous nannofossils and planktonic foraminifers. Because little previous work has been done on the late Cenozoic biostratigraphy of the subtropical eastern North Atlantic, the primary biostratigraphic aim was to calibrate the dinocyst biostratigraphy against the calcareous nannofossil and planktonic foraminifer biostratigraphies, rather than to challenge or revise these. Reworking, suggested, for example, by the presence of the Miocene marker *Sumatradinium hispidum* in Pliocene-Pleistocene sediments in Hole 898A, made the assignment of ages to some samples difficult. In other cases, well preserved specimens were present in sediments assigned an age which is older than the published FAD for that species; the middle Miocene palynomorph *Incertae sedis* I of Edwards 1984, for instance, was found in sediments assigned an early Miocene age in Holes 898A and 900A. This suggests either that the FAD of this palynomorph must be revised, or that the age assigned to these sediments is too old. Dinocyst assemblages also provide insight into surface water mass characteristics. Through much of the late Cenozoic a *Lingulodinium machaerophorum*-*Operculodinium israelianum*/*O. crassum* assemblage characterized the Iberia Abyssal Plain. Except for a brief interval during the late Miocene, when sparse *Impagidinium*-*Spiniferites* dominated assemblages are found in sediments from Hole 900A, *Lingulodinium machaerophorum* and *Operculodinium israelianum*/*O. crassum* were common components of the microflora deposited over 11 m.y., from middle Miocene Zone NN7 until early Pleistocene Zone NN19C. The interruption of this microflora during the late Miocene suggests that the Mediterranean was isolated from the North Atlantic at that time, interrupting the transport of *Lingulodinium machaerophorum* and *Operculodinium israelianum*/*O. crassum* cysts onto the Iberia Abyssal Plain in the Mediterranean overflow. It also supports the argument that the dominance of *Impagidinium* spp. in oceanic sediments may be primarily because of the absence of other cysts (cf. Zonneveld, 1995).

During the early Pleistocene, the *L. machaerophorum-Operculodinium israelianum/O. crassum* microflora was again replaced, this time by a *Bitectatodinium tepikiense-Spiniferites* spp.-*Operculodinium centrocarpum* microflora. This records the existence of cooler surface waters off Iberia (?or perhaps in the Mediterranean) since approximately 1.4 Ma. A similar change in dinocyst assemblages at this time off New Jersey has been related to climatically induced intensification of the Gulf Stream (McCarthy, 1992), which would be expected to affect the entire subtropical gyre.

Although ODP Sites 898 and 900 are only 43 km apart, and differ bathymetrically only by 242.2 m, their Pliocene-Pleistocene palynological records differ markedly. The lower D:P ratios at Site 898 probably result from the abundant influx of terrigenous sediments transported onto the abyssal plain by turbidity currents. Terrigenous sediments appear to have bypassed Site 900, at the base of the continental rise. Turbidites in Hole 898A can be identified palynologically by their low D:P (ratio of marine vs. terrestrial palynomorphs), and by the presence of *Brigantedinium* cysts (and accompanying low G:P ratios). The presence of *Brigantedinium* cysts in turbidites is consistent with their initiation during glacioeustatic sea level lowstands because this genus has been associated with colder, lower salinity surface water (Mudie and Short, 1985).

SYSTEMATIC NOTES

Palynological specimens are curated at the Atlantic Geoscience Centre, Bedford Institute of Oceanography; curation numbers and England finder references are given in Plate captions. The classification of dinoflagellates follows Fensome et al. (1993). All formal names follow the nomenclatural index of Lentin and Williams (1993), where synonyms are given.

Division PYRRHOPHYTA Pascher 1914
Class DINOPHYCEAE Fritsch 1929
Genus *ACHOMOSPHERA* Evitt, 1963

Achomosphaera andalusiensis Jan du Chêne, 1977
emend. Jan du Chêne and Londeix, 1988
(Plate 3, Fig. 7)

Remarks: Most specimens of this species in Holes 898A and 900A have two or more complex, reticulated process tips, typical of the upper Miocene holotype of Jan du Chêne (1977). Some middle Miocene specimens, however, are not clearly distinguishable from *A. callosa* Matsuoka, 1983 and *A. ramosasimilis* (Yun, 1981) Londeix et al., 1992, which are reported from upper and lower Pliocene sediments of the Mediterranean (Benzakour, 1992). It is notable that *A. andalusiensis* shows cyclical high abundances in Pleistocene sediments at the study sites, in the northwest Atlantic (ODP Site 647 and survey site 89007-11), and in the subtropical Gulf of California (Byrne et al., 1990); these abundance peaks are strongly correlated with early interglacials, suggesting that this species prefers warm, relatively low salinity (melt-water/fluvial) conditions.

Achomosphaera ramulifera (Deflandre) Evitt, 1963
(Plate 3, Fig. 8)

A well-known species, usually with a LAD in the late Pliocene, but rarely present or redeposited in lower Pleistocene deposits at many North Atlantic sites (e.g., Mudie, 1987; 1989; de Vernal and Mudie, 1989).

Genus *AMICULOSPHERA* Harland 1979
Amiculosphaera umbracula Harland, 1979
(Plate 3, Fig. 18)

This distinctive species is found in Pliocene-Pleistocene sediments in Holes 898A and 900A. This species has been reported from upper Miocene through early Pleistocene sediments at northeast Atlantic Sites 400, 607, 611, and 642 (Harland, 1979; Mudie 1987, 1989), but it is not known from the northwest Atlantic Ocean or Mediterranean Sea.

Genus *APTEODINIUM* Eisenack, 1958
Apteodinium australiense (Deflandre and Cookson, 1955) Williams, 1978
(Plate 1, Fig. 5)

Specimens assigned to this species are large proximochorate cysts (diameter >60 µm) with a well-developed apical horn, a well-defined wide paracingulum, and a non-cavernous finely spongy-granulate wall. In the North Atlantic, *A. australiense* has a mid-middle Miocene LAD (Williams et al., 1993); it has not been reported for the Mediterranean.

Apteodinium? sp. A Powell 1986b
(Plate 1, Fig. 1)

Specimens from both Holes 898A and 900A resemble the species from lower Miocene sediments of the Italian Lemme Section, as illustrated by Powell (pl. 6, fig. 3; 1986b). *Apteodinium?* sp. A is a pear-shaped to ovoidal autocyst, with a low apical horn and an irregularly alveolate cyst wall, the surface of which is sparsely papillate. The paracingulum is indicated by low obtuse ridges; the archeopyle is precingular. This species is distinguished from *A. spiridoides* and from the late middle Miocene species *Apteodinium* sp. 1 of Head et al., 1989c by its smaller size (diameter ~50 µm), by the well-defined paracingulum and the finer alveolate ornament and presence of papillae.

Apteodinium spiridoides Benedek, 1972
(Plate 1, Fig. 6)

Specimens are large (diameter ~80 µm) and cavernous, without visible paratabulation or apical horn. The outer cyst wall is ornamented by large irregular alveoli and scattered verrucae. This species has a HO (highest occurrence) at or below the early/middle Miocene boundary at most North Atlantic sites although there are also a few reports for the early middle Miocene (Head et al., 1989c), and Haq et al. (1988) correlated the highest occurrence of this species to the early middle Miocene biozones NN5 and N10. *A. spiridoides* differs from the related species *Apteodinium tectatum* in its thick fibrous (cancellous) outer wall structure (see Head and Wrenn, 1992).

Genus *BATIACASPHAERA* Drugg, 1970
Batiacasphaera sphaerica Stover 1977
(Plate 1, Fig. 7)

Specimens assigned to this species were consistently rounded and relatively thick-walled, with uniformly papillate surfaces, and are distinct from smaller crumpled cysts that may belong to the *B. micropapillata* Stover, 1977 "complex" described by Head et al., 1989c. *B. sphaerica* has an early to late Miocene range in the North Atlantic (Head et al., 1989c).

Genus *BITECTATODINIUM* Wilson, 1973
Bitectatodinium tepikiense Wilson, 1973
(Plate 4, Fig. 10; Plate 5, Figs. 5, 6)

This cyst is abundant in modern sediments where it is well preserved and clearly shows the distinctive camerate archeopyle associated with the loss of two dorsal precingular paraplates at excystment, and the sub-erect branching lamellate nature of the periphragm ornament which arises from raised bases, as described by Head (1994a). On the Iberia Abyssal Plain, *B. tepikiense* is only abundant in late Pliocene and younger sediments. Rare specimens in Miocene sediments are larger, with thicker walls and denser, less regularly oriented lamellae.

Genus *BRIGANTEDINIUM* Reid, 1974
Brigantedinium spp.
(Plate 4, Fig. 6)

Round or oblong cysts with a dark brown wall color, pentagonal archeopyle and absence of surface ornament, are assigned as *Brigantedinium* species. Many cysts could be ascribed to either *B. simplex* (Wall, 1965) Reid, 1977 (see Pl. 4, Fig. 6) or to *B. cariacoense* (Wall, 1967) Reid, 1977, but other forms could not be identified at the species level due to damaged/hidden archeopyle areas.

Genus *CALIGODINIUM* Drugg, 1970
Caligodinium pychnum Biffi and Manum, 1988
(Plate 1, Fig. 9)

Specimens from the Iberia Abyssal Plain are large (75 × 30 µm), with a coarsely reticulate epiphragm and cone-shaped verrucae, closed at the tips, and closely resemble early Miocene cysts from the northwest Atlantic (Williams and Bujak, 1977). Specimens from the Mediterranean late Oligocene to early Miocene (Brinkhuis et al., 1992) are broader and less elongate in shape,

with a finer reticulate ornament. *C. pychnum* has a HO in early Miocene sediments of the North Atlantic (Williams et al., 1993) and the Mediterranean region (Brinkhuis et al., 1992).

Genus *CANNOSPHAEROPSIS* O. Wetzel, 1933, emend. Williams and Downie, 1966
Cannosphaeropsis cf. *C. utinensis* O. Wetzel, 1933 sensu Brown and Downie, 1986
 (Plate 2, Fig. 10)

In Holes 898A and 900A, early Miocene specimens resembling *C. utinensis* have long processes with periphragm trabeculae in the paracingular region and a finely punctate endophragm. Similar specimens have been found in lower Eocene through upper Miocene sediments of the North Atlantic region, and according to Head and Wrenn (1992), this cyst form is now recognized as a species distinct from *C. utinensis* O. Wetzel, 1933 sensu Brown and Downie, 1986. It is being studied by L. de Verteuil who refers to the species as *Cannosphaeropsis* "passio" (G.L. Williams, pers. comm., 1995).

Genus *CHIROPTERIDIUM* Gocht, 1960
Chiropteridium mespilanum (Maier, 1959) Lentin and Williams 1973
 (Plate 2, Fig. 13)

Poorly preserved specimens of this species are not easily distinguished from the Oligocene-early Miocene species *C. partispinosum*. Specimens from the Iberia Abyssal Plain, however, are relatively small and resemble illustrations of *C. mespilanum* from Miocene sections in Italy (Powell, 1986a,b).

Genus *CORRUDINIUM* Stover and Evitt, 1978
Corrudinium harlandii Matsuoka, 1983
 (Plate 4, Fig. 20)

This species is rare in upper Miocene sediments of Hole 900A.

Genus *CYCLOPSIELLA*
Cyclopsiella granosa (Matsuoka 1983) Head et al., 1992
 (Plate 1, Fig. 11)

Specimens with granulate ornamentation are occasionally present in lower Miocene sediments in Holes 898A and 900A, and are assigned to *C. granosa*. This species has an early middle Eocene to middle Miocene range in the North Atlantic and has been reported from the Pleistocene in Australia (Head and Wrenn, 1992). It appears to be characteristic of warm-water regions (see Head and Wrenn, 1992).

Genus *DAPSILIDINIUM* Bujak et al., 1980
Dapsilidium pastielsii (Davey and Williams, 1966) Bujak et al., 1980
 (Plate 1, Fig. 2)

This species is common in the lower Miocene sediments from the Iberia Abyssal Plain, together with *D. pseudocolligerum*, from which it usually differs by its more rigid, conical spines, with small flared tips and broad bases. However, there may be intergrades between these two taxa.

Dapsilidium pseudocolligerum (Stover, 1977) Bujak et al., 1980
 (Plate 1, Fig. 12)

This species is common in lower Miocene sediments from the Iberia Abyssal Plain and typically has long, relatively weak, simple or bifurcate processes (up to 1/3 body width). The process tips are often bent or recurved, and always have flared distally open tips. However, there may be intergrades with *D. pastielsii*.

Dapsilidium sp. of Wrenn and Kokinos, 1986
 (Plate 1, Fig. 10)

Middle late Miocene and early Pliocene specimens resembling *D. pseudocolligerum* but with smaller, with short, variable processes may be the species illustrated by Wrenn and Kokinos from the Gulf of Mexico (pl. 10, figs. 8-10; 1986).

Genus *DISTATODINIUM* Eaton, 1976
Distatodinium paradoxum (Brosius, 1963) Eaton, 1967
 (Plate 2, Fig. 4)

This species is rare in lower Miocene samples from the Iberia Abyssal Plain; this is consistent with its reported LAD in the earliest Miocene of the North Atlantic (Williams et al., 1993).

Genus *FILISPHAERA* Bujak, 1984 emend. Head in Head, 1994b
Filisphaera filifera Bujak, 1984, emend. Head in Head, 1994b
 (Plate 2, Figs. 14, 15; Plate 4, Fig. 9)

Brownish cysts with a microreticulate periphragm of narrow septa and precingular archeopyle were assigned to this species, which also includes rare Pliocene forms with pilose ornament of radiating fibres (*F. filifera* ssp. *pilosa*). *F. filifera* has a late Miocene to earliest Pleistocene distribution in the North Atlantic (Head, 1994) but this cool-water species (Versteegh and Zonneveld, 1994) is rare and poorly preserved in middle Miocene and late Pliocene sediments at Site 898 and may be reworked. *F. filifera* ssp. *pilosa* has a Pliocene range in the Bering Sea (Head, 1994b) and North Atlantic Site 611 (Mudie, 1987).

Genus *GALEACYSTA* Corradini and Biffi, 1988
Galeacysta etrusca Corradini and Biffi, 1988
 (Plate 2, Fig. 12)

Specimens assigned to this species are rare and poorly preserved, suggesting possible reworking; however, this cyst may be a marker of transport in Mediterranean overflow water.

Genus *HABIBACYSTA* Head et al., 1989b
Habibacysta cf. *H. tectata* Head et al., 1989b
 (Plate 4, Fig. 5; Plate 5, Fig. 8, 10)

Cysts resembling *H. tectata* are rare in Hole 898A, and few of them have a clearly visible archeopyle. Some forms, however, were found with an attached opercular paraplate, which distinguishes them from the Labrador Sea topotypes (Head et al., 1989b) and Norwegian Sea specimens (Mudie, 1989). The Iberia Abyssal Plain cyst form may be more similar to the Gulf of Mexico cyst *Tectatodinium* sp. A of Wrenn and Kokinos (1986; pl. 5, fig. 3) which has an attached operculum. This cyst form and *Tectatodinium* sp. II of de Vernal and Mudie, 1989 from Hole 898A (see Pl. 4, Fig. 14) need SEM study to define the exact nature of the ectophragm structure.

Genus *HOMOTRYBLIUM* Davey and Williams, 1966
Homotryblium floripes (Deflandre and Cookson, 1955) Stover, 1975
 (Plate 2, Fig. 8)

These cysts showed a large variability in process development, particularly with respect to the length and width of the large hollow processes. Some intergradation with the contemporary populations of *H. oceanicum* and *H. vallum* and/or *H. tenuispinosum* may account for this variation. *H. floripes* has an Oligocene to late early Miocene range in the North Atlantic (Williams et al., 1993).

Homotryblium oceanicum Eaton, 1976
 (Plate 2, Fig. 3)

Only a few strongly oxidized specimens of this species were found in lower Miocene sediments. This species is restricted to the Eocene at most North Atlantic sites (Williams and Bujak, 1985) and is probably reworked on the Iberia Abyssal Plain.

Homotryblium tenuispinosum Davey and Williams, 1966
 (Plate 1, Fig. 3)

Specimens assigned to this category differ from *H. floripes* in having longer, thinner processes. This species is rare and may be reworked from Paleogene sediments.

Homotryblium vallum Stover, 1977
 (Plate 2, Fig. 7)

This species occurs in lower Miocene sediments in Holes 898A and 900A, which is consistent with its late Oligocene to late early Miocene range in the North Atlantic (Williams et al., 1993).

Genus *HYSTRICHOKOLPOMA* Klumpp, 1953, emend. Williams and Downie, 1966

Hystrichokolpoma cinctum Klumpp, 1953
(Plate 3, Fig. 16)

This species is rare in lower Miocene sediments in Holes 898A and 900A; it has a middle early Miocene LAD in the North Atlantic according to Williams et al. (1993).

Hystrichokolpoma rigaudiae Deflandre and Cookson, 1955
(Plate 2, Fig. 6)

This species has a Paleogene through lower Pliocene range in the North Atlantic (Williams et al., 1993) and is present in Italian Pliocene sections (Habib, 1971; Powell, 1986c).

Genus *HYSTRICHOSPHEROPSIS* Deflandre, 1935
Hystrichosphaeropsis obscura Habib, 1972
(Plate 3, Fig. 13)

Few, poorly preserved specimens of this species were found in lower Miocene sediments in Hole 900A. Smaller, well-preserved specimens occur in the middle Miocene and upper Pliocene at both sites.

Genus *IMPAGIDINIUM* Stover and Evitt, 1978
Impagidinium aculeatum (Wall) Lentin and Williams, 1981
(Plate 4, Fig. 12)

There is a notable decrease in the size of this well-known species from its first occurrence in the middle Miocene to Pleistocene sediments in both Holes 898A and 900A. Miocene specimens have a typical size of ~50 X 45 µm compared to ~35 X 30 µm in Pliocene-Pleistocene sediments.

Impagidinium aliferum Mudie, 1987
(Plate 4, Fig. 11)

This species is probably often overlooked and counted as *I. aculeatum* although its larger body size (55 × 30-35 µm) and expanded (4-8 µm) parasutural crests are consistently distinctive. This species has a Pliocene range at the Iberia Abyssal Plain sites and at DSDP Site 607 west of the Azores. At DSDP Site 611 south of Iceland, its range extends to the upper Miocene (Mudie, 1987).

Impagidinium aspinatum (Cookson and Eisenack, 1974) Damassa, 1979
(Plate 5, Fig. 1)

Specimens ascribed to this species occur in the lower Miocene of Hole 898A and resemble *Impagidinium* sp. cf. *I. aspinatum* of Powell (1986b) as illustrated for lower Miocene sediments at the Italian Lemme section. Both Lemme and Iberia Abyssal Plain specimens are dark in color, suggesting possible reworking of the Paleogene species *I. aspinatum*.

Impagidinium bacatum Londeix et al., 1992
(Plate 4, Fig. 4; Plate 5, Fig. 9)

This species is rare in upper Pliocene sediments in Hole 900A; this is consistent with its acme in the Mediterranean in the upper Pliocene (Benzakour, 1992; Londeix et al., 1992). Under light microscopy, it is difficult to distinguish *I. bacatum* from the Mesozoic *I. pentahedrias*, and the Paleogene species *I. aspinatum*, and some specimens assigned to *I. bacatum* may be reworked Cretaceous cysts.

Impagidinium patulum (Wall, 1967) Stover and Evitt, 1978
(Plate 4, Fig. 21)

This well-known species has its FAD in the early Miocene in Hole 898A, but its acme occurs in middle Pleistocene sediments in Hole 898A, and in upper Miocene to lower Pliocene sediments in Hole 900A, where it may form almost monospecific assemblages. Very little variation in size or morphology has been observed in the Iberia Abyssal Plain, central North Atlantic and Mediterranean samples (Mudie, 1987; Aksu et al., 1995), in contrast to the size variation in Miocene sediments reported by Edwards (1984) and by Head et al. (1989b).

Impagidinium sphaericum (Wall, 1967) Stover and Evitt, 1978
(Plate 4, Fig. 25)

This species appears much later (Pliocene) in the eastern North Atlantic than *I. patulum* with which it is sometimes confused. The two taxa are easily distinguished by the smaller size and more rounded body of *I. sphaericum*, and its very low or missing parasutural crests.

Impagidinium sp. A of Mudie, 1987
(Plate 4, Figs 22a and 22b)

These small *Impagidinium* cyst forms appear to be the same as those described and illustrated from samples studied in the subtropical and subarctic N. Atlantic (Mudie, 1987) and the arctic Labrador and Norwegian Seas (Mudie, 1987; 1989), where they are abundant in the lower Pliocene sediments. In the Iberia Abyssal Plain cores, however, they have their acme in the late Pliocene.

Impagidinium sp. F Wrenn and Kokinos, 1986
(Plate 4, Fig. 18)

This species is not always easily distinguishable from, and may include, specimens of *I. japonicum* Matsuoka, 1983 (Plate 4, Fig. 13).

Genus *INVERTOCYSTA* Edwards, 1984
Invertocysta lacrymosa Edwards, 1984
(Plate 3, Fig. 15)

Specimens of *I. lacrymosa* from Miocene sediments were often poorly preserved, in contrast to common occurrences of well-preserved cysts in upper Pliocene sediments at both sites. Rare specimens of *I. tabulata* (Plate 2, Fig. 2) were also seen in Miocene and Pliocene sediments.

Genus *LABYRINTHODINIUM*
Labyrinthodinium truncatum Piasecki, 1980
(Plate 4, Fig. 29)

Specimens of this middle Miocene marker are rare in the Iberia Abyssal Plain sediments and well preserved cysts were found only in Hole 900A. This species has a late early Miocene to early late Miocene range in the North Atlantic (Head et al., 1989b), but it has not previously been reported for the Mediterranean region and it was not reported by Harland (1979) for DSDP Site 400 off the Bay of Biscay.

Genus *LEJEUNECYSTA* Artzner and Dorhofer, 1978 emend. Lentin and Williams, 1976
Lejeunecysta communis Biffi and Grignani, 1983
(Plate 4, Fig. 17)

Poorly preserved (oxidized) specimens are rare in upper Pliocene-Pleistocene samples in Hole 898A, but not in Hole 900A, although the species is common in Pliocene sediments of the Mediterranean (Biffi and Grignani, 1983) and the outer shelf off Newfoundland (Mudie, pers. observation). Some of these specimens may be conspecific with *L. marieae* Harland in Harland et al. (1991) which is common in upper Pliocene deltaic and paralic sites, as at the St. Erth beds (Head, 1993).

Genus *LINGULODINIUM* Wall, 1967 emend. Dodge 1989
Lingulodinium machaerophorum (Deflandre and Cookson, 1955) Wall, 1967
(Plate 3, Fig. 1)

This is the most common species throughout both sites on the Iberia Abyssal Plain, yet it shows relatively little morphological change from Miocene to Pleistocene, and all excysted specimens showed almost complete loss of all epicystal paraplates, with only the sulcal paraplate remaining attached. In general, Miocene specimens have relatively short blade-shaped processes, or rarely, very short, club-shaped processes. In contrast, most Pliocene-Pleistocene specimens had long, flexuous blade-shaped processes. These morphological variations may be related to different paleoenvironmental conditions as noted in Head (1993).

Genus *MELITASPHAERIDIUM* Harland and Hill, 1979
Melitasphaeridium choanophorum (Deflandre and Cookson, 1955)
Harland and Hill, 1979
(Plate 4, Fig. 28)

In Hole 898A, well-preserved specimens of this cyst form are rare in the Pliocene to early Pleistocene interval, but fragments of process tips resem-

bling those of the species may indicate reworking. This species is found in upper Miocene sediments in Hole 900A.

Genus *MULTISPINULA* Bradford, 1975

Multispinula? minuta Harland and Reid in Harland et al., 1980

This species is questionably included in the genus *Algidasphaeridium* by Lentin and Williams (1993) who list it as *Algidasphaeridium? minutum* (Harland and Reid in Harland et al., 1980) Matsuoka and Bujak, 1988, a species described as having a chasmic archeopyle. Paratype specimens from the Beaufort Sea were studied by Mudie (1992) and these clearly have an intercalary rather than chasmic archeopyle, so we retain the generic name *Multispinula* at this time.

Multispinula quanta Bradford, 1975

This species is present at both sites, but it is most common in lower Pleistocene sediments from Hole 898A.

?*Multispinula* sp.
(Plate 4, Fig. 8)

Specimens are small brown cysts (body diameter 30–35 µm) with short, solid spines ~1/4 of the body length and expanded process tips. A pentagonal archeopyle outline was seen in some specimens.

Multispinula sp. of Wrenn and Kokinos, 1986
(Plate 3, Fig. 2)

These cysts are similar to *M. quanta*, but much larger (75 µm maximum body diameter) and with wider (>2µm) spine-bearing paracingular margins.

Genus *NEMATOSPHAEROPSIS* Deflandre and Cookson, 1955
emend. Williams and Downie, 1966
Nematosphaeropsis labyrinthus (Ostenfeld, 1903) Reid, 1974
(Plate 4, Fig. 15)

Specimens with the typical features of this species (as shown in Plate 4) appear only in the Pliocene-Pleistocene sediments on the Iberia Abyssal Plain. Similar cysts in older sediments are smaller and crumpled, so they could not be assigned with certainty to either *Nematosphaeropsis* or *Cannosphaeropsis*.

Nematosphaeropsis major Head et al., 1989a
(Plate 3, Fig. 19)

Well-preserved specimens of this species are rare in lower Miocene sediments in Hole 898A and in middle Miocene sediments in Hole 900A.

Nematosphaeropsis oblonga Mudie, 1987
(Plate 4, Figs. 23, 24)

Specimens of this middle Miocene-late Pliocene species are very similar to those found at DSDP Sites 607 and 611 in the central North Atlantic (Mudie, 1987). This species is also found in Pliocene sediments of Site 647, Labrador Sea (de Vernal and Mudie, 1989), and it may overlap with some morphotypes of *Nematosphaeropsis* sp. 1 of Head et al., 1989b from the upper Miocene of the Labrador Sea, which also has rod-like trabeculae and an elongate body with finely granular surface ornament. *Nematosphaeropsis oblonga* consistently differs in morphology from *N. lemniscata*, even within the same populations as seen at Sites 611 and 607 in the N. Atlantic, and it is clearly a separate species despite the opinion of Wrenn (1988), as discussed in Head and Wrenn (1992).

Genus *OPERCULODINIUM* Wall, 1967
Operculodinium centroparium (Deflandre and Cookson) Wall, 1967
(Plate 3, Fig. 17)

The literature contains a high diversity of morphotypes that have been assigned to this species. Miocene specimens resemble the Australian holotype which are larger and more robust than modern specimens; this morphotype is rare in Holes 898A and 900A. Pliocene and Pleistocene specimens at the two sites closely resemble the species in modern and Pliocene-Pleistocene sedi-

ments of the Atlantic, Arctic, and Mediterranean regions, and have relatively long processes (~half body diameter), of uniform length and with bifurcate tips.

Operculodinium crassum Harland, 1979
(Plate 3, Fig. 10)

Recently Harland (in Head and Wrenn, 1992) opined that *O. crassum* and *O. israelianum* are synonymous, with *O. crassum* the junior homonym. Study of the abundant specimens in the Iberia Abyssal Plain cores, however, and knowledge of the range of morphology in Pleistocene Mediterranean sediments (Aksu et al., 1995) leads to the conviction that there are two species. *O. crassum* has a thick wall (2–4 µm) and sturdy spines at least one-third of the body diameter, while *O. israelianum* (Plate 3, Fig. 9) has a thinner wall and shorter spines, ~one-tenth of the body diameter. The two taxa are almost co-dominant in lower Pliocene sediments, but *O. crassum* is dominant or exclusively present in older sediments, and *O. israelianum* dominates in the Pleistocene sediments.

Operculodinium? eirikianum Head et al., 1992
(Plate 3, Fig. 12)

Specimens of this species are easily distinguished from poorly preserved specimens of *O. longispinum* primarily by the microreticulate wall ornament and shorter (<10 µm) processes. Characteristic features of Iberia Abyssal Plain specimens of *O. eirikianum* are the recurved processes which are variable in length, with several different tip shapes, ranging from bifurcate to acute or acuminate, and the strongly microreticulate wall ornament.

Operculodinium israelianum (Rossignol) Wall, 1967
(Plate 3, Fig. 9)

See notes for *O. crassum*.

Operculodinium janduchenei Head et al., 1992
(Plate 4, Fig. 1; Plate 5, Fig. 7)

The processes in this species are very variable in length and morphology (Head et al., 1989a). In this study, only specimens with sturdy conical spines and apparently closed tips were assigned to this species.

Genus *PALAEOCYSTIDIINIUM*
Palaeocystidinium golzowense Alberti, 1961
(Plate 1, Fig. 4)

This species is rare in the lower Miocene sediments from the Iberia Abyssal Plain. This distribution contrasts with the common occurrence of this species in middle through upper Miocene sediments in the northern North Atlantic (Head et al., 1989b; Mudie, 1989).

Genus *PENTADINIUM* Gerlach, 1961 emend. Benedek et al., 1982
Pentadinium laticinctum Gerlach, 1961 emend. Benedek et al., 1982
(Plate 2, Fig. 5)

Genus *POLYSPHAERIDIUM* Davey and Williams, 1966; emend. Bujak et al., 1980
Polysphaeridium congregatum (Stover, 1977) Bujak et al. 1980
(Plate 3, Fig. 6)

This species, which is rare in lower Miocene sediments in Holes 898A and 900A, has an Oligocene to early Miocene range in most of the North Atlantic (G.L. Williams, pers. comm, 1995), but it is not present in Baffin Bay (Head et al., 1989c), Labrador Sea (Head et al., 1989b), or the Norwegian Sea (Manum et al., 1989).

Polysphaeridium zoharyi (Rossignol, 1962) Bujak et al., 1980

This species is common throughout the Iberia Abyssal Plain sections, but shows greater morphological variation in lower Miocene sediments were *P. zoharyi* subsp. *ktana* (Rossignol) Lentin and Williams 1981 is present.

Genus *PYXIDIELLA* Cookson and Eisenack, 1958
Pyxidiella? simplex Harland, 1979
(Plate 4, Figs. 2, 16; Plate 5, Fig. 3)

This species includes a wide range of small oblong cysts with granulose to verrucose ornament and an apparently intercalary archeopyle. Two cyst forms are present in middle Miocene sediments in Hole 900A. Most specimens have a slightly elongate apical boss and predominantly conate ornamentation (Plate 4, Fig. 2; Plate 5, Fig. 3) and they appear similar to the late Miocene species described by Harland (1979). Other specimens have a more rounded shape (Plate 4, Fig. 16), predominantly granulate ornament, and the archeopyle is large, with a pentagonal outline; this morphotype more closely resembles the cyst form from middle to upper Miocene sediments at DSDP Site 555, Rockall Plateau (Edwards, 1984), which was referred to as *Tectatodinium simplex* (Harland) Edwards 1984.

Genus *RETICULATOSPHERA* Matsuoka, 1983 emend. Bujak and Matsuoka, 1986

Reticulatosphaera actinocoronata (Benedek, 1972) Bujak and Matsuoka, 1986

This species is occasionally present in middle Miocene through upper Pliocene samples at both Sites 898 and 900. This species has a late Eocene to early Pliocene range in the North Atlantic (Head et al., 1989b).

Genus *SELENOPEMPHIX* Benedek, 1972 emend. Head, 1993

Selenopemphix nephroides Benedek, 1972 emend. Bujak, 1980
(Plate 3, Figs 3, 5; Plate 4, Fig. 3)

Pliocene and early Pleistocene specimens attributed to this species are often crumpled and cannot equivocally be assigned to this species (Plate 4, Fig. 3). Some well-preserved specimens (Plate 3, Fig. 3) show an archeopyle slightly offset to the right side of the cyst, and smooth paracingular margins. Similar variation of archeopyle symmetry was found in specimens of *S. nephroides* in upper Pliocene samples from southwest England (Head, 1993). Other specimens in Hole 898A have an almost symmetrical archeopyle (Plate 3, Fig. 5) and serrate wing ornament similar to that found in the late Miocene to lower Pliocene species *Selenopemphix brevispinosa* Head et al., 1989c. *S. nephroides* is common through the late Pliocene and early Pleistocene of the northeast Atlantic, although it disappears in the early Pleistocene in the northwest Atlantic (de Vernal and Mudie, 1989).

Genus *SPINIFERITES* Mantell, 1850 emend. Sarjeant, 1970

Spiniferites mirabilis (Rossignol) Sarjeant, 1970
(Plate 4, Fig. 27; Plate 5, Fig. 4)

This species appears to occur throughout the section at both sites; however, there is a change in the morphology of the compound antapical process and in the length of the gonal processes. Miocene specimens tend to have relatively short spines, with one posterior spine only partly fused to the compound process, in contrast to Pliocene-Pleistocene specimens that have fully fused antapical processes and longer, more branched gonal processes.

Spiniferites ramosus (Ehrenberg) Loeblich and Loeblich, 1966

This taxon includes specimens assigned by other workers to *Spiniferites bulloideus* (Deflandre and Cookson) Sarjeant, 1970, since there appears to be complete gradation between both forms in the samples studied.

Spiniferites splendidus Harland, 1979
(Plate 4, Fig. 26)

Spiniferites spp.

This category includes unknown taxa similar to *S. ramosus*/*S. mirabilis* and broken/obscured/poorly preserved cysts obviously attributable to this genus, but which could not be identified to species level were counted as *Spiniferites* sp. The group may include some species of the genus *Achomospaera* Evitt, 1963.

Genus *STELLADINIUM* Bradford, 1975

Stelladinium stellatum (Wall and Dale, 1968) Reid, 1977
(Plate 4, Fig. 19)

Specimens of this species are rare and usually poorly preserved in the Pliocene-Pleistocene sediments in Hole 898A and are absent from Hole 900A.

Genus *SUMATRADINIUM* Lentin and Williams, 1976

Sumatradinium druggii Lentin et al., 1994
(Plate 3, Fig. 11)

Specimens assigned to this *Sumatradinium* species showed a very wide range of process length and tip branches; more than one species may be present in the middle Miocene to lower Pliocene sediments at both Iberia Abyssal Plain sites, although the Pliocene specimens may be reworked.

Sumatradinium hispidum Lentin et al., 1994

(Plate 3, Fig. 11)

This species was found only in late Pliocene sediments in Hole 898A. It is distinguished, with difficulty, from short-spined forms of *Multispinula? minuta* by its larger size (>60 µm) and granuloreticulate wall ornament. According to Head (1994b), the genus *Sumatradinium* has its LAD in the late Miocene; hence the Pliocene specimens may be reworked.

Genus *TECTATODINIUM* Wall, 1967

Tectatodinium pellitum Wall, 1967

This species is rare in early Miocene through Pleistocene sediments on the Iberia Abyssal Plain. Early Miocene specimens in Sample 149-898A-28X-2, 58-60 cm are large (~70 µm, slightly compressed) with walls ~5 µm thick, falling in the uppermost range of specimens studied by Head (1994a). Pliocene-Pleistocene specimens have a diameter ~60 µm and wall thickness of 3 µm.

Tectatodinium sp. II of de Vernal and Mudie, 1989

(Plate 4, Fig. 14)

See comments for *Habibacysta*.

Genus *THALASSIPHORA* Eisenack and Gocht, 1960

Thalassiphora delicata Williams and Downie, 1966
(Plate 2, Fig. 11)

Specimens of this species usually appeared thin-walled and oxidized: it is not clear if they are redeposited but their occurrence at both Iberia Abyssal Plain sites suggest that they are autochthonous.

Thalassiphora pelagica Eisenack and Gocht, 1960

(Plate 5, Fig. 2)

Specimens resembling this cyst form were rare and poorly preserved in lower Miocene sediments from both Iberia Abyssal Plain sites.

Thalassiphora cf. *T. pansa* of Mudie, 1989

(Plate 2, Fig. 1)

This cyst form showed a wide range in development of the protruding periphragm structures that characterize *T. pansa*; some specimens more closely resembled the middle Miocene Dinocyst sp. 7 of Manum et al., 1989.

Genus *TUBERCULODINIUM* Wall, 1967

Tuberculodinium vancampoeae (Rossignol, 1962) Wall, 1967
(Plate 1, Fig. 8)

Specimens of this species are often smaller in Miocene sediments than in upper Pliocene sediments where larger specimens similar to modern cyst forms were common in Hole 898A.

ACKNOWLEDGMENTS

We acknowledge the laboratory assistance of Shelley Thibaudau, Mary Jo Mittelholtz, Ted Little, and Bill Parkins, and the assistance of Mike Lozon in producing figures. This work was supported by an NSERC operating grant to F. McCarthy and AGC Project 820044 funds to P. Mudie. Discussions with Martin Head, Graham Williams, Rob Fensome, and Anne de Vernal were valuable, as were the insights and data of Eric Collins and other members of the Ship-

board Scientific Party, L. Liu, E. de Kaenel, D. Milkert, E. Gervais. This paper greatly benefited from helpful critical reviews by Martin Head and Rex Harland.

REFERENCES

- Aksu, A.E., Yaar, D., Mudie, P.J., and Gillespie, H., 1995. Late glacial-Holocene paleoclimatic and paleoceanographic evolution of the Aegean Sea: micropaleontological and stable isotope evidence. *Mar. Micropaleontol.*, 25:1-28.
- Benzakour, M., 1992. Les paléoenvironnements marins de la Méditerranée centrale Néogène Supérieure par l'analyse des kystes de dinoflagellés [Ph.D. thesis]. Univ. du Québec, Montréal.
- Biffi, U., and Grignani, D., 1983. Peridinioid dinoflagellate cysts from the Oligocene of the Niger delta, Nigeria. *Micropaleontology*, 29:126-145.
- Brinkhuis, H., Powell, A.J., and Zevenboom, D., 1992. High resolution dinoflagellate cyst stratigraphy of the Oligocene/Miocene transition interval in Northwest and Central Italy. In Head, M.J., and Wrenn, J.H. (Eds.), *Neogene and Quaternary Dinoflagellate Cysts*. Am. Assoc. Stratigr. Palynol. Contrib., 19:219-258.
- Byrne, R., Mudie, P.J., and Soutar, A., 1990. A pollen/dinoflagellate chronology for Site 480, Gulf of California. In Betancourt, J.L., and MacKay, A.M. (Eds.), *Proc. 6th Ann. Pacific Climate (PACLIM) Workshop*, 1989:105-110.
- Cita, M.B., 1979. Lacustrine and hypersaline deposits in the desiccated Mediterranean and their bearing on paleoenvironment and paleo-ecology. In Talwani, M., Hay, W., and Ryan, W.B.F. (Eds.), *Deep Drilling Results in the Atlantic Ocean: Continental Margins and Paleoenvironment*. Am. Geophys. Union, 402-419.
- Corradini, D., and Biffi, U., 1988. Etude des dinokystes à la limite Messinien-Pliocène dans la coupe Cava Serridi, Toscane, Italie. *Bull. Cent. Rech. Explor.-Prod. Elf-Aquitaine*, 12:221-236.
- Costa, L.I., and Downie, C., 1979. Cenozoic cyst stratigraphy of Sties 403 to 406, Rockall Plateau, Leg 48, Deep Sea Drilling Project. In Montadert, L., Roberts, D.G., et al., *Init. Repts. DSDP*, 48: Washington (U.S. Govt. Printing Office), 513-529.
- Dale, B., 1976. Cyst formation, preservation, and sedimentation: factors affecting dinoflagellate assemblages in Recent sediments from Trondhemsfjord, Norway. *Rev. Paleobot. Palynol.*, 22:39-60.
- de Vernal, A., Londeix, L., Mudie, P.J., Harland, R., Morzadec-Kerfourn, M.T., Turon, J.-L., and Wrenn, J.H., 1992. Quaternary organic-walled dinoflagellate cysts of the North Atlantic Ocean and adjacent seas: ecostratigraphy and biostratigraphy. In Head, M.J., and Wrenn, J.H. (Eds.), *Neogene and Quaternary Dinoflagellate Cysts*. Am. Assoc. Stratigr. Palynol. Contrib., 289-328.
- de Vernal, A., and Mudie, P.J., 1989. Pliocene and Pleistocene palynostratigraphy at ODP Sites 646 and 647, eastern and southern Labrador Sea. In Srivastava, S.P., Arthur, M.A., Clement, B., et al., *Proc. ODP, Sci. Results*, 105: College Station, TX (Ocean Drilling Program), 401-422.
- Dietrich, G., 1963. *General Oceanography*: New York (Interscience).
- Dodge, J.D., 1994. Biogeography of marine armoured dinoflagellates and dinocysts on the NE Atlantic and North Sea. *Rev. Paleobot. Palynol.*, 84:169-180.
- Dodge, J.D., and Harland, R., 1991. The distribution of planktonic dinoflagellates and their cysts in the eastern and northeastern Atlantic Ocean. *New Phytol.*, 118:593-603.
- Edwards, L.E., 1984. Miocene dinocysts from Deep Sea Drilling Project Leg 81, Rockall Plateau, Eastern North Atlantic Ocean. In Roberts, D.G., Schnitker, D., et al., *Init. Repts. DSDP*, 81: Washington (U.S. Govt. Printing Office), 581-594.
- Edwards, L.E., Mudie, P.J., and de Vernal, A., 1991. Pliocene paleoclimatic reconstruction using dinoflagellate cysts: comparison of methods. *Quat. Sci. Rev.*, 10:259-274.
- Fairbridge, R.W. (Ed.), 1966. *Encyclopedia of Oceanography*: New York (Van Nostrand Reinhold).
- Fensome, R.A., Taylor, F.J.R., Norris, G., Sarjeant, W.A.S., Wharton, D.I., and Williams, G.L., 1993. A classification of living and fossil dinoflagellates. *Micropaleontol., Spec. Publ.*, 7.
- Habib, D., 1971. Dinoflagellate stratigraphy across the Miocene-Pliocene boundary, Tabiano stratotype section. In Farinacci, A. (Ed.), *Proc. 2nd Int. Conf. Planktonic Microfossils Roma*: Rome (Ed. Tecnosci.), 1:591-598.
- Haq, B.U., Hardenbol, J., and Vail, P.R., 1988. Mesozoic and Cenozoic chronostratigraphy and cycles of sea-level change. In Wilgus, C.K., Hastings, B.S., Kendall, C.G.St.C., Posamentier, H.W., Ross, C.A., and Van Wagoner, J.C. (Eds.), *Sea-Level Changes—An Integrated Approach*. Spec. Publ.—Soc. Econ. Paleontol. Mineral., 42:72-108.
- Harland, R., 1977. Recent and late Quaternary (Flandrian and Devensian) dinoflagellate cysts from marine continental shelf sediments around the British Isles. *Paleontographica B*, 164:87-126.
- , 1979. Dinoflagellate biostratigraphy of Neogene and Quaternary sediment at Holes 400/400A in the Bay of Biscay (Deep Sea Drilling Project Leg 48). In Montadert, L., Roberts, D.G., et al., *Init. Repts. DSDP*, 48: Washington (U.S. Govt. Printing Office), 531-545.
- , 1983. Distribution maps of recent dinoflagellate cysts in bottom sediments from the North Atlantic Ocean and adjacent seas. *Palaeontology*, 26:321-387.
- , 1989. A dinoflagellate cyst record for the last 0.7 Ma from the Rockall Plateau, northeast Atlantic Ocean. *J. Geol. Soc. London*, 146:945-951.
- , 1992. Dinoflagellate cysts of the Quaternary System. In Powell, A.J. (Ed.), *A Stratigraphic Index of Dinoflagellate Cysts*: London (Chapman Hall), Br. Micropaleontol. Soc. Publ. Ser.
- Harland, R., Bonny, A.P., Hughes, M.J., and Morigi, A.N., 1991. The lower Pleistocene stratigraphy of the Ormesby Borehole, Norfolk, England. *Geol. Mag.*, 128:647-660.
- Head, M.J., 1993. Dinoflagellates, sporomorphs, and other palynomorphs from the Upper Pliocene St. Erth Bed of Cornwall, southwestern England. *J. Paleontol. (Suppl.)* 67:1-62 (also *Paleontol. Soc. Mem.*, 31).
- , 1994a. Morphology and paleontological significance of the Cenozoic dinoflagellate genera *Tectatodinium* and *Habibacysta*. *Micropaleontology*, 40:289-321.
- Head, M.J. (Ed.), 1994b. A forum on Neogene and Quaternary dinoflagellate cysts (The edited transcript of a round table discussion held at the Third Workshop on Neogene and Quaternary Dinoflagellates; with taxonomic appendix). *Palynology*, 17:201-239.
- Head, M.J., Matsuoka, K., and Mudie, P.J., 1992. Nomenclatural note on the Neogene marine acritarch *Cyclopsiella granosa* (Matsuoka, 1983) Head et al., comb. nov. In Head, M.J., and Wrenn, J.H. (Eds.), *Neogene and Quaternary Dinoflagellate Cysts*. Am. Assoc. Stratigr. Palynol. Contrib., 163-164.
- Head, M.J., Norris, G., and Mudie, P.J., 1989a. New species of dinocysts and a new species of acritarch from the Upper Miocene and Lowermost Pliocene, ODP Leg 105, Site 646, Labrador Sea. In Srivastava, S.P., Arthur, M.A., Clement, B., et al., *Proc. ODP, Sci. Results*, 105: College Station, TX (Ocean Drilling Program), 453-466.
- , 1989b. Palynology and dinocyst stratigraphy of the upper Miocene and lowermost Pliocene, ODP Leg 105, Site 646, Labrador Sea. In Srivastava, S.P., Arthur, M.A., Clement, B., et al., *Proc. ODP, Sci. Results*, 105: College Station, TX (Ocean Drilling Program), 423-451.
- , 1989c. Palynology and dinocyst stratigraphy of the Miocene in ODP Leg 105, Hole 645E, Baffin Bay. In Srivastava, S.P., Arthur, M.A., Clement, B., et al., *Proc. ODP, Sci. Results*, 105: College Station, TX (Ocean Drilling Program), 467-514.
- Head, M.J., and Wrenn, J.H. (Eds.), 1992. A forum on Neogene and Quaternary dinoflagellate cysts (The edited transcript of a round table discussion held at the Third Workshop on Neogene and Quaternary Dinoflagellates). In Head, M.J., and Wrenn, J.H. (Eds.), *Neogene and Quaternary Dinoflagellate Cysts*. Am. Assoc. Stratigr. Palynol. Contrib., 1-31.
- Jan du Chêne, R., 1977. Etude palynologique du Miocène supérieure Andalous (Espagne). *Rev. Espan. Micropaleontol.*, 9:97-114.
- Kaneps, A.G., 1979. Gulf Stream: velocity fluctuations during the late Cenozoic. *Science*, 204:297-301.
- Lentin, J.K., and Williams, G.L., 1993. Fossil dinoflagellates: index to genera and species, 1993 edition. *Am. Assoc. Stratigr. Palynol., Contrib.*, 28:1-856.
- Londeix, L., Benzakour, M., and de Vernal, A., 1992. *Impagidinium bacatum*, a new dinoflagellate species from the Mediterranean Pliocene: systematics, biostratigraphy and Paleoecology. *Geobios*, 25:695-702.
- Manum, S.B., Boulter, M.C., Gunnarsdottir, H., Rangnes, K., and Scholze, A., 1989. Eocene to Miocene palynology of the Norwegian Sea (ODP Leg 104). In Eldholm, O., Thiede, J., Taylor, E., et al., *Proc. ODP, Sci. Results*, 104: College Station, TX (Ocean Drilling Program), 611-662.
- McCarthy, F.M.G., 1992. Quaternary climate change and the evolution of the mid-latitude western North Atlantic Ocean: palynological, foraminiferal, sedimentological, and stable isotope evidence from DSDP Sites 604, 607 and 612 [Ph.D. thesis]. Dalhousie University, Halifax.

- Miller, K.G., Fairbanks, R.G., and Mountain, G.S., 1987. Tertiary oxygen isotope synthesis, sea-level history, and continental margin erosion. *Paleoceanography*, 2:1-19.
- Mudie, P.J., 1987. Palynology and dinoflagellate biostratigraphy of Deep Sea Drilling Project Leg 94, Sites 607 and 611, North Atlantic Ocean. In Ruddiman, W.F., Kidd, R.B., Thomas, E., et al., *Init. Repts. DSDP*, 94 (Pt. 2): Washington (U.S. Govt. Printing Office), 785-812.
- , 1989. Circum-Arctic Quaternary and Neogene marine palynofloras: Paleocology and statistical analysis. In Head, M.J., and Wrenn, J.H. (Eds.), *Neogene-Holocene Dinoflagellate Cysts*. Am. Assoc. Stratigr. Palynol. Contrib., 347-390.
- Mudie, P.J., de Vernal, A., and Head, M.J., 1990. Neogene to Recent palynostratigraphy of Circum-Arctic basins: results of ODP Leg 104, Norwegian Sea, Leg 105, Baffin Bay, and DSDP Site 611, Irminger Sea. In Bleil, U., and Thiede, J. (Eds.), *Proc. 1988 NATO Adv. Res. Workshop on Geological History of the Polar Oceans: Arctic vs. Antarctic*. NATO ASI Ser., Ser. C, 308:609-646.
- Mudie, P.J., and McCarthy, F.M.G., 1994. Late Quaternary pollen transport processes, western North Atlantic: data from box models, cross-margin and N-S transects. *Mar. Geol.*, 118:79-105.
- Mudie, P.J., and Short, S.K., 1985. Marine palynology of Baffin Bay. In Andrews, J.T. (Ed.), *Quaternary Environments*: London (Allen and Unwin).
- Pickard, G.L., and Emery, W.J., 1982. *Descriptive Physical Oceanography* (4th ed.): New York (Pergamon Press).
- Powell, A.J., 1986a. A dinoflagellate cyst biozonation for the late Oligocene to middle Miocene succession of the Langhe region, northwest Italy. In Wrenn, J.H., Duffield, S.L., and Stein, J.A. (Eds.), *Papers from the First Symposium on Neogene Dinoflagellate Cyst Biostratigraphy*. Am. Assoc. Stratigr. Palynol. Contr. Ser., 17:105-127.
- , 1986b. Latest Paleogene and earliest Neogene dinoflagellate cysts from the Lemme section, northwest Italy. In Wrenn, J.H., Duffield, S.L., and Stein, J.A. (Eds.), *Pap. 1st Symp. Neogene Dinoflagellate Cyst Biostratigraphy*. Am. Assoc. Stratigr. Palynol. Contrib., 17:83-104.
- , 1986c. The stratigraphic distribution of late Miocene dinoflagellate cysts from the Castellanian Superstage Stratotype, northwest Italy. In Wrenn, J.H., Duffield, S.L., and Stein, J.A. (Eds.), *Pap. 1st Symp. Neogene Dinoflagellate Cyst Biostratigraphy*. Am. Assoc. Stratigr. Palynol. Contrib., 17:129-149.
- , 1992. A Stratigraphic Index of Dinoflagellate Cysts: London (Chapman Hall), Br. Micropaleontol. Soc. Publ. Ser.
- Shipboard Scientific Party, 1994a. Introduction. In Sawyer, D.S., Whitmarsh, R.B., Klaus, A., et al., *Proc. ODP, Init. Repts.*, 149: College Station, TX (Ocean Drilling Program), 5-10.
- , 1994b. Site 898. In Sawyer, D.S., Whitmarsh, R.B., Klaus, A., et al., *Proc. ODP, Init. Repts.*, 149: College Station, TX (Ocean Drilling Program), 115-146.
- , 1994c. Site 900. In Sawyer, D.S., Whitmarsh, R.B., Klaus, A., et al., *Proc. ODP, Init. Repts.*, 149: College Station, TX (Ocean Drilling Program), 211-262.
- Stockmarr, J., 1971. Tablets with spores used in absolute pollen analysis. *Pollen et Spores*, 13:615-621.
- Sy, A., 1988. Investigation of large scale circulation patterns in the central North Atlantic: the North Atlantic Current, Azores Current, and the Mediterranean Water plume in the area of the Mid Atlantic Ridge. *Deep Sea Res. Part A*, 35:383-413.
- Turon, J.L., 1984. Le phytoplancton dans l'environnement actuel de l'Atlantique nord oriental. Evolution climatique et hydrologique depuis le dernier maximum glaciaire. *Mem. Inst. Geol. Bassin Aquitaine*, 17.
- Versteegh, G.J.M., and Zonneveld, K.A.F., 1994. Determination of (palaeo)ecological preferences of dinoflagellates by applying detrended and canonical correspondence analysis to late Pliocene dinoflagellate cyst assemblages of the south Italian Singa section. *Rev. Paleobot. Palynol.*, 84:181-199.
- Wall, D., Dale, B., Lohmann, G.P., and Smith, W.K., 1977. The environmental and climatic distribution of dinoflagellate cysts in modern marine sediments from regions in the North and South Atlantic Oceans and adjacent seas. *Mar. Micropaleontol.*, 2:121-200.
- Williams, G.L., and Bujak, J.P., 1977. Cenozoic palynostratigraphy of offshore eastern Canada. *Am. Assoc. Stratigr. Palynol. Contrib.*, 5A: 14-47.
- Williams, G.L., Stover, L.E., and Kidson, E.J., 1993. *Morphology and Stratigraphic Ranges of Selected Mesozoic-Cenozoic Dinoflagellate Taxa in the Northern Hemisphere*. Pap.—Geol. Surv. Can., 92-10.
- Wrenn, J.H., 1988. Differentiating species of the dinoflagellate cyst genus *Nematosphaeropsis* Deflandre and Cookson 1955. *Palynology*, 12:129-150.
- Wrenn, J.H., and Kokinos, J.P., 1986. Preliminary comments on Miocene through Pleistocene dinoflagellate cysts from De Soto Canyon, Gulf of Mexico. In Wrenn, J.H., Duffield, S.L., and Stein, J.A. (Eds.), *Am. Assoc. Stratigr. Palynol. Contrib.*, 17:169-225.
- Zonneveld, K.A.F., 1995. Palaeoclimatic and palaeo-ecological changes during the last deglaciation in the Eastern Mediterranean—implications for dinoflagellate ecology. *Rev. Paleobot. Palynol.*, 84:221-253.

Date of initial receipt: 5 December 1994

Date of acceptance: 8 August 1995

Ms 149SR-256

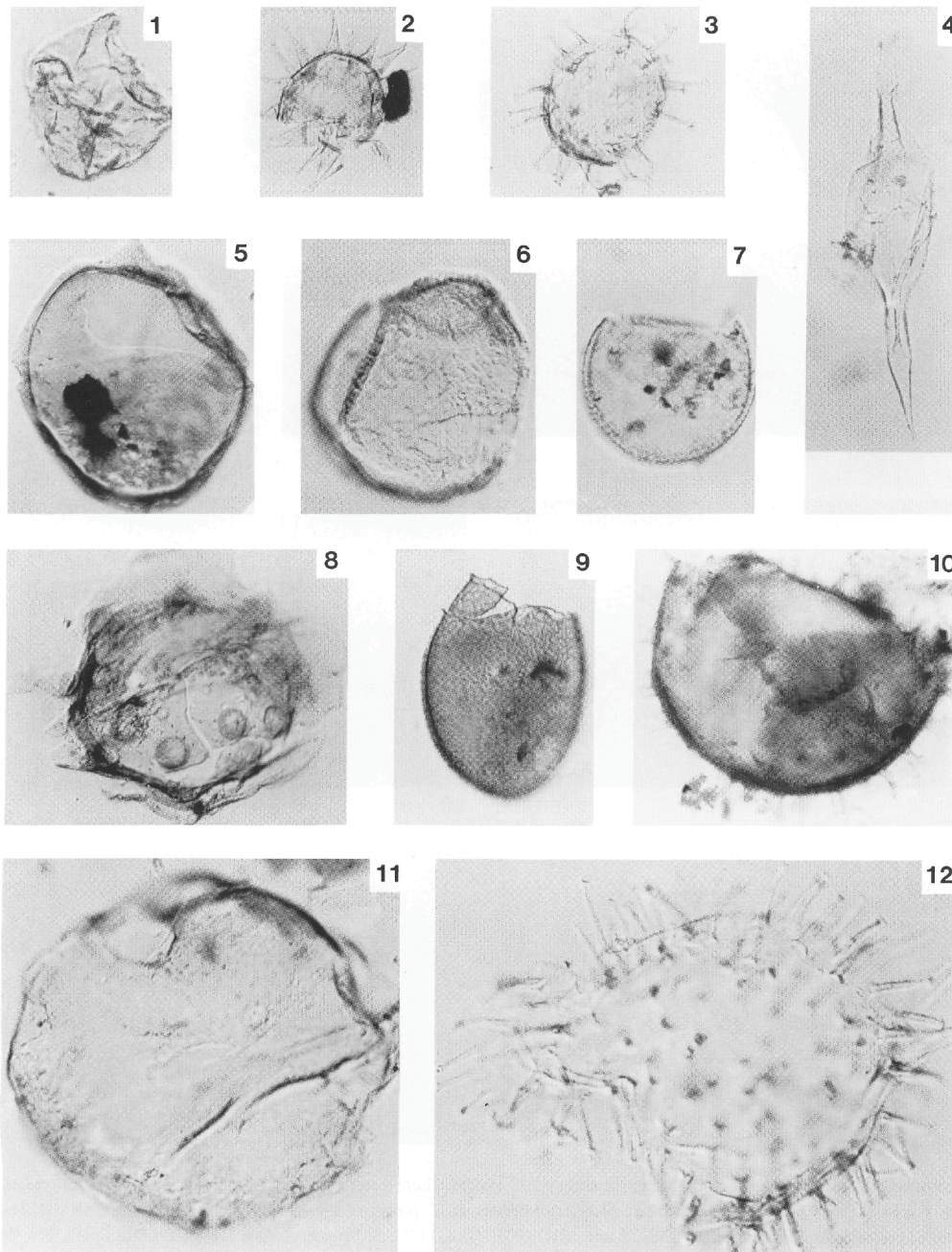


Plate 1. Interference contrast microscope photographs (magnification $\times 292$ except 7, 10-12, which are $\times 730$) of selected early-middle Miocene dinocysts. AGC curation and England Finder references are in parentheses. HI, MID, and LO are focal planes. **1.** *Apteodinium?* sp. A. of Powell, 1986b: Sample 900A-36R-3B, 95-97 cm; HI (951329, G22/0). **2.** *Dapsilidinium pastielsii*: Sample 898A-23X-4A, 100-103 cm; HI (951012, V38/4). **3.** *Homotryblium tenuispinosum*: Sample 898A-23X-4A, 100-103 cm; HI (951215, U34/1). **4.** *Palaeocystodinium golzowense*: Sample 900A-21R-1A, 101-103 cm; MID (951332, X27/0). **5.** *Apteodinium australiense*: Sample 898A-25X-2, 74-76 cm (Slide 2); HI (950923, 033/0). **6.** *Apteodinium spiridoides*: Sample 898A-25X-2, 74-76 cm (Slide 2); MID (950922, P21/0). **7.** *Batiacasphaera sphaerica*: 898A-25X-2, 74-76 cm; MID, (950920, V29/2). **8.** *Tuberculodinium vancampoae*: 898A-25X-2, 74-76 cm; MID (950925; L35/2). **9.** *Caligodinium pychnum*: Sample 898A-23X-4A, 100-103 cm; HI (951034; D28/4). **10.** *Dapsilidinium* sp. of Wrenn and Kokinos, 1986: Sample 898A-18X-5, 60-63 cm; LO (940924, M22/0). **11.** *Cyclopsiella granosa*: Sample 898A-23X-4A, 100-103 cm; HI (951006, X37/2). **12.** *Dapsilidinium pseudocolligerum*: Sample 898A-28X-2, 58-60 cm; MID (940943, Y38/3).

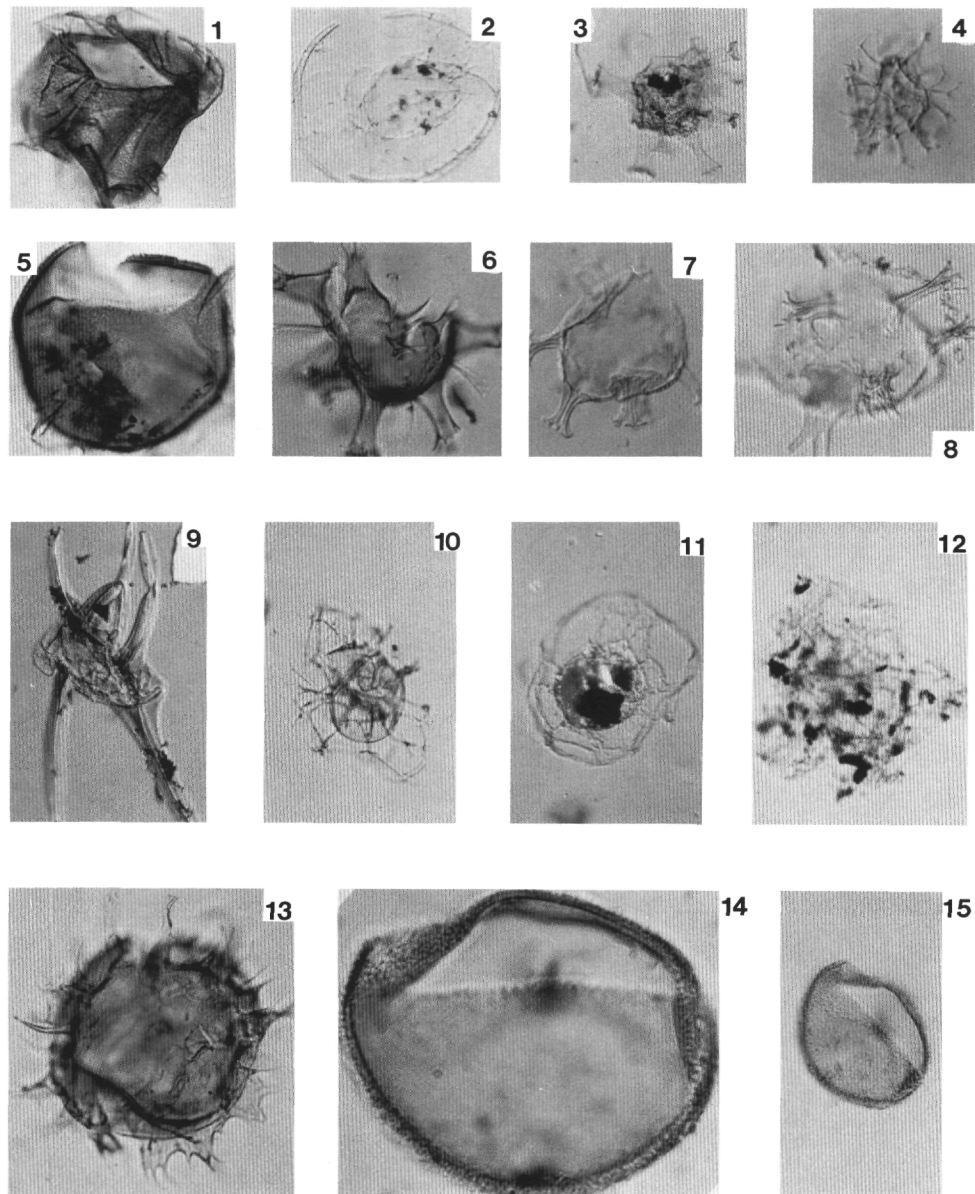


Plate 2. Interference contrast microscope photographs (magnification $\times 292$ except where noted) of selected dinocysts. AGC curation and England Finder references in parentheses. HI, MID, and LO are focal planes. **1.** *Thalassiphora* sp. cf. *T. pansa* of Mudie, 1989: Sample 898A-28X-2D, 16-18 cm; HI (941112, X18/1). **2.** *Invertocysta tabulata*: Sample 900A-10R-4, 31-33 cm; MID (941210, Q11/3). **3.** *Homotryblium oceanicum*: Sample 898A-23X-4B, 100-103 cm; HI (951115, 0320). **4.** *Distatodinium paradoxum*: Sample 898A-28X-2C, 16-18 cm; MID (941115, 019/3). **5.** *Pentadinium laticinctum*: Sample 898A-28X-2C, 16-18 cm; MID (941111, Q31/0). **6.** *Hystriocholpoma rigaudiae*: Sample 898A-28X-2B, 16-18 cm; HI (941107, R46/0). **7.** *Homotryblium vallum*: Sample 898A-28X-2B, 16-18 cm; MID (950927, W41/0). **8.** *Homotryblium floripes*: Sample 898A-28X-2B, 16-18 cm; MID (950926, W27/2). **9.** Incertae sedis I of Edwards, 1984: Sample 900A-10R-4, 31-33 cm; HI (941214; D18/3). **10.** *Cannosphaeropsis* cf. *C. utinensis*: Sample 898A-28X-2, 58-60; HI (940949; N32/0). **11.** *Thalassiphora delicata*: Sample 898A-19X-1, 40-42 cm; HI (940906, K19/0). **12.** *Galeacysta etrusca*: Sample 900A-10R-4, 141-143 cm; HI (941211; Q25/4). **13.** *Chiropteridium mespilanum*: Sample 898A-28X-2C, 58-60 cm; HI (940955, T31/0). **14, 15.** *Filisphaera filifera*: Sample 898A-13H-1, 85-87 cm. (951411, L40/2). 14. MID $\times 730$. 15. HI $\times 292$.

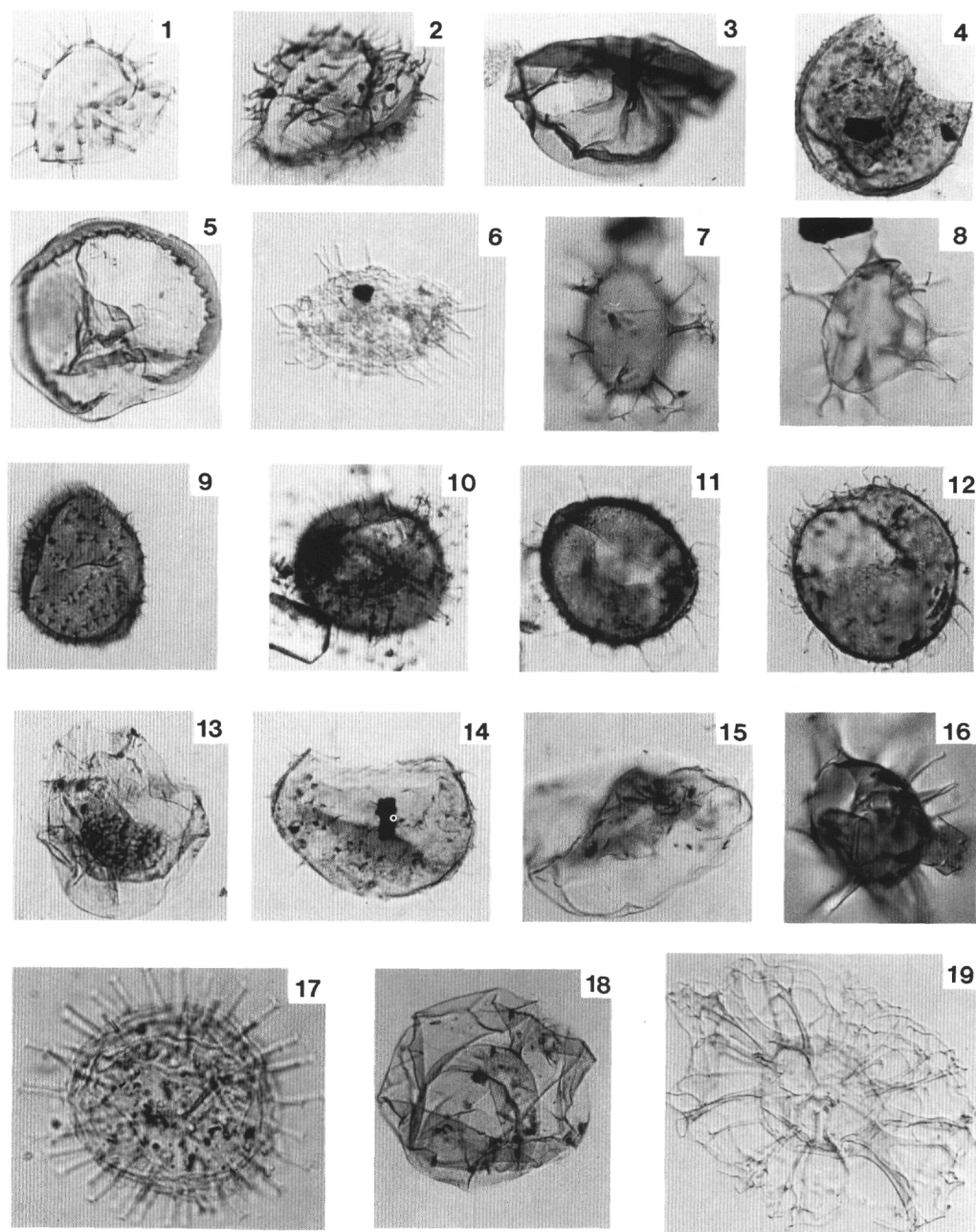


Plate 3. Interference contrast microscope photographs ($\times 292$ except where noted) of selected dinocysts. AGC curation and England Finder references in parentheses. HI, MID, and LO are focal planes. **1.** *Lingulodinium machaerophorum*: Sample 898A-18X-2, 16-18 cm; MID (940979, V17/3). **2.** *Multispinula* sp. of Wrenn and Kokinos, 1986: 898A-18X-2, 16-18 cm; MID (940980, V81/1). **3.** *Selenopemphix nephroides*: 898A-18X-2, 16-18 cm; HI (940986, F33/0). **4.** *Sumatradinium hispidum*: 898A-18X-2, 16-18 cm; HI (940981, T12/4). **5.** *Selenopemphix brevispinosa*: Sample 898A-5H-5, 87-89 cm; HI (951412, N33/0). **6.** *Polysphaeridium congregatum*: 898A-23X-4A, 100-103 cm; HI (951022, J9/2). **7, 8.** Sample 898A-1H-6A, 3-5 cm. **7.** *Achomospaera andalusiensis*; HI (941164, R26/3). **8.** *Achomospaera ramulifera*; HI (941167, M25/0). **9.** *Operculodinium israelianum*: Sample 900A-18R-2, 58-60 cm; HI (940988, X22/1). **10.** *Operculodinium crassum*: Sample 898A-18X-CC; MID (940971, M27/3). **11.** *Sumatradinium druggii*: Sample 898A-18X-2, 16-18 cm; HI (940984, J16/3). **12.** *Operculodinium?* *eirikianum*: Sample 900A-18R-2, 16-18 cm; MID (940989, X22/1). **13.** *Hystrichosphaeropsis obscura*: Sample 898A-6H-5A, 98-100 cm; HI (951404, X44/4). **14.** *Sumatradinium* sp.: Sample 898A-18X-2, 16-18 cm. HI (940984). **15.** *Invertocysta lacrymosa*: Sample 900A-17R-1, 92-94 cm; MID (921146, D29/3). **16.** *Hystrichokolpoma cinctum*: Sample 898A-28X-2C, 58-60 cm; HI (941117, L24/2). **17.** *Operculodinium centrocarpum*: Sample 898A-18X-2, 16-18 cm; MID, $\times 730$ (940982, R46/0). **18.** *Amiculosphaera umbracula*: Sample 900A-18R-2A, 58-60 cm; HI (941131, D16/2). **19.** *Nematosphaeropsis major*: Sample 898A-22X-4, 113-115 cm; HI (951123, G8/0).

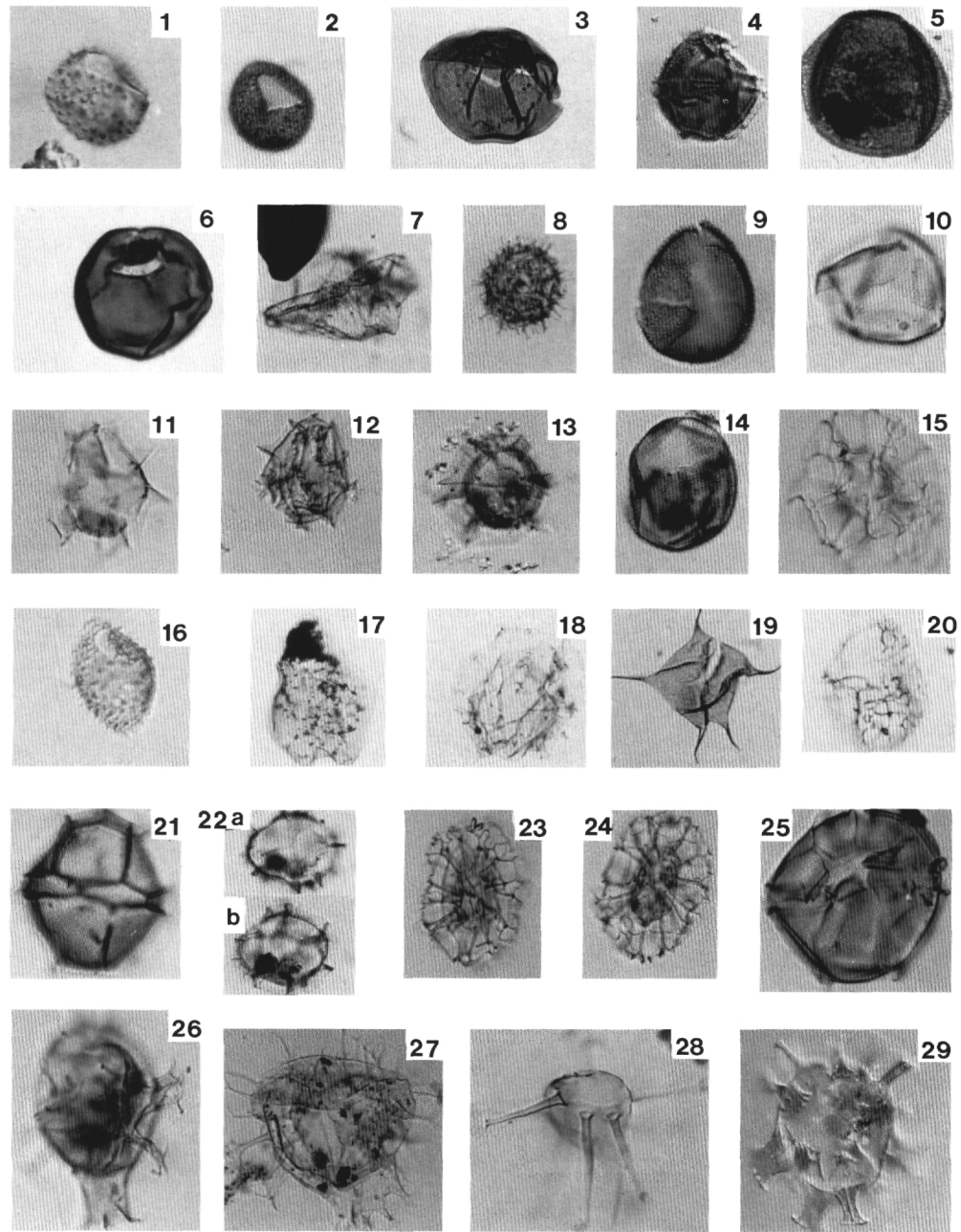


Plate 4. Interference contrast microscope photographs of selected dinocysts ($\times 29$). AGC curation and England Finder references in parentheses. HI, MID, and LO are focal planes. **1.** *Operculodinium janduchenei*: Sample 898A-1H-6B, 3-5 cm; HI (941171, V46/2). **2.** *Pyxidiella? simplex*: Sample 900-18R-2, 58-60 cm; HI (940913, Y30/1). **3-5.** Sample 898A-1H-6B, 3-5 cm. **3.** *Selenopemphix* cf. *S. nephroides*; HI (940976, Y11/0). **4.** *Impagidinium bacatum*; MID (941114, C22/2). **5.** *Habibacysta tectata*; MID (940968, E18/3). **6.** *Brigantedinium simplex*: Sample 898A-5H-5, 87-89 cm; HI (941157, P32/0). **7.** *Selenopemphix* sp.: Sample 898A-1H-6B, 3-5 cm; MID (941152, R40/0). **8.** ?*Multispinula* sp.: Sample 898A-13H-1, 85-87; MID (941119A, V42/0). **9.** *Filisphaera filifera*: Sample 898A-1H-6A, 3-5 cm; MID (941115, N25/0). **10, 11.** Sample 898A-17X-1 A, 92-93 cm. **10.** *Bitectatodinium tepikiense*; HI (941111, X30/2). **11.** *Impagidinium aliferum*; MID (941116, V42/2). **12.** *Impagidinium aculeatum*: Sample 898A-18X-4A, 63-66 cm; HI (941174, X24/2). **13.** *Impagidinium japonicum* Matsuoka, 1983: Sample 898A-16X-1, 29-31; MID (941123, Q28/2). **14.** *Tectatodinium* sp. II of de Vernal and Mudie, 1989: Sample 898A-17x-1A, 92-93; MID (941113, W34/3). **15.** *Nematosphaeropsis labyrinthus*: Sample 900A-18R-2, 58-60 cm; HI (941118). **16.** *Pyxidiella* sp. of Edwards, 1984: Sample 900-18R-2, 13-15 cm; MID (940904, 823/2). **17.** *Lejeunecysta communis*: Sample 898A-13X-4, 140-143 cm; MID (941220, X19/0). **18.** *Impagidinium* sp. F of Wrenn and Kokinos, 1986: Sample 898A-17X-2, 141-143 cm; MID (941218, V42/0). **19.** *Stelladinium stellatum*: Sample 898A-5H-5, 87-89 cm; HI (941301, D25/3). **20.** *Corrudinium harlandii*: Sample 900A-16R-5, 81-83 cm; HI (941202, M16/3). **21, 22.** Sample 900A-18R-2, 58-60 cm. **21.** *Impagidinium patulum*; HI (941102, N43/3). **22.** *Impagidinium* sp. A of Mudie, 1987: a = HI (941142, M46/1); b = MID (941143, M46/1). **23, 24.** *Nematosphaeropsis oblonga*: Sample 900A-18R-2A, 58-60 cm. **23.** HI (941103, 012/3). **24.** MID (941104, 012/3). **25.** *Impagidinium sphaericum*: Sample 898A-1H-6B, 3-5 cm; (941180, H30/2). **26.** *Spiniferites splendidus*: Sample 898A-1H-6B, 3-5 cm; MID (941108). **27.** *Spiniferites mirabilis/hyperacanthus* of Benzakour, 1992: Sample 900A-18R-2, 58-60; MID (940987, X20/3). **28.** *Melitasphaeridium choanophorum*: Sample 898A-1H-6B, 3-5 cm; MID (941122, S41/0). **29.** *Labyrinthodinium truncatum*: Sample 900-18R-2, 13-15 cm; MID (941123).

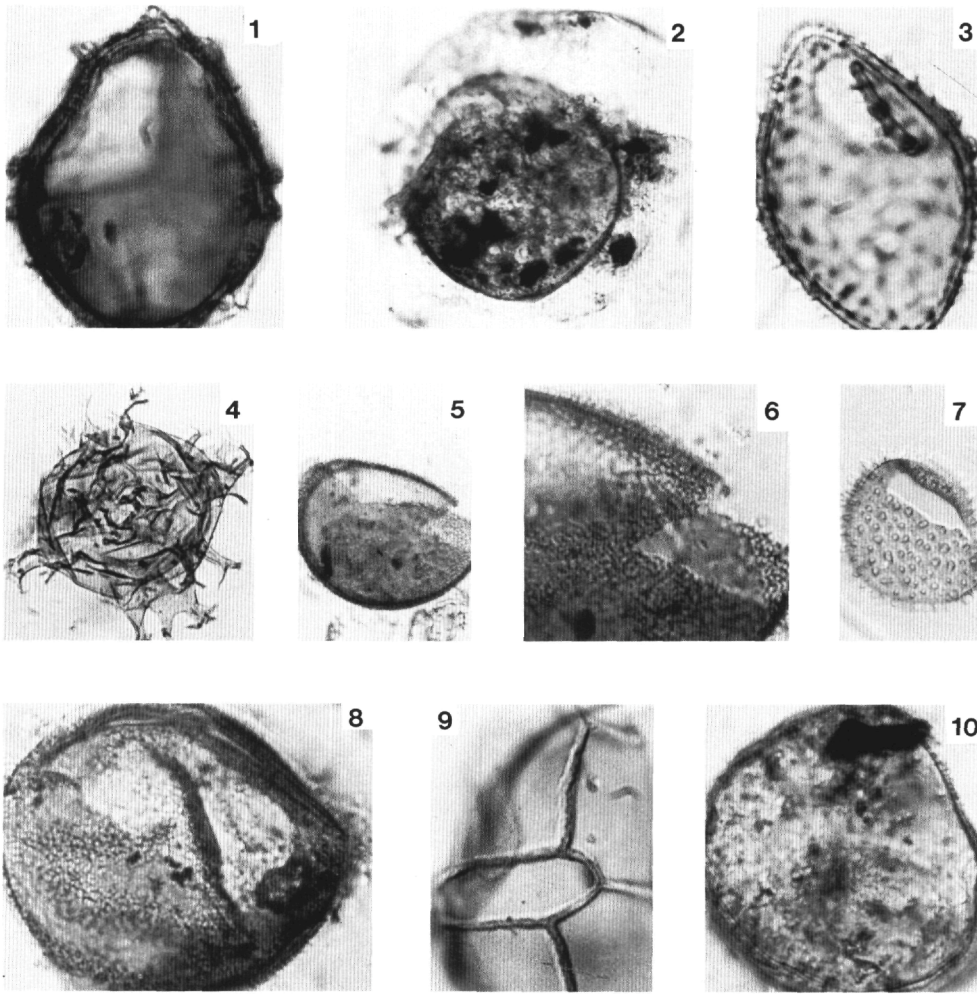


Plate 5. Interference contrast microscope photographs of selected dinocysts. AGC duration and England Finder references in parentheses. HI, MID, LO are focal planes. **1.** *Impagidinium aspinatum*: Sample 898A-28X-2C, 58-60 cm; MID $\times 730$ (941123, W15/1). **2.** *Thalassiphora pelagica*: Sample 898A-28X-2C, 16-18 cm; HI $\times 29$ (941124). **3, 4.** Sample 900-18R-2, 58-60 cm. **3.** *Pyxidiella? simplex*; MID $\times 730$ (940913, Y30/1). **4.** *Spiniferites mirabilis*; MID (940987, X20/0). **5, 6.** Sample 898A-18R-CC. *Bitectatodinium tepikiense*; **5.** MID, $\times 292$. **6.** HI, $\times 730$. **7.** *Operculodinium janduchenei*: Sample 898A-28X-2B, 58-60 cm; HI $\times 292$ (950929, M17/3). **8.** *Habibacysta tectata*: Sample 898A-1R-CC; MID $\times 730$ (951308, K22/0). **9.** *Impagidinium bacatum*: Sample 900A-16R-5, 81-83 cm; HI (941208, X41/4). **10.** *Habibacysta tectata*: Sample 898A-19X-1, 40-42 cm; MID $\times 730$ (951314, F18/0).